Crustal Evolution of the Egyptian Precambrian Rocks

4

Robert J. Stern and Kamal Ali

Contents

Abstract

Precambrian basement of the Egyptian sector of the Arabian-Nubian Shield are well exposed on the flanks of the Red Sea and along the border with Sudan, making it an excellent place to study Neoproterozoic processes of crustal growth, obduction–accretion tectonics, and post collisional escape tectonics. We review the published field observations, structural geological analyses, and geochemical and isotopic data to provide an up-to-date overview Neoproterozoic and pre-Neoproterozoic crustal formation in Egypt. Egyptian basement exposures are distributed in three major places: southern Sinai, the Eastern Desert and in the southernmost Western Desert. Neoproterozoic igneous rocks dominate basement exposures in southern Sinai, the Eastern Desert, and the eastern part of the SW Desert, although ~1.0 Ga crust is documented from northernmost basement exposures in southern Sinai. Neoproterozoic basement rocks mainly consist of ophiolite associations, calc-alkaline and alkaline, and immature sediments; these rocks are especially well exposed in the Central Eastern Desert. Older Neoproterozoic basement rocks represent juvenile arc terranes that formed during Upper Tonian–Cryogenian time at ~650–750 Ma around the margins of the Mozambique Ocean. Accretion of juvenile arc and backarc basin systems ended by Late Neoproterozoic time (~620 Ma) when large fragments of east and west Gondwana collided, closing the Mozambique Ocean and forming the East African-Antarctic Orogen. Orogenic collapse and escape tectonics to form NW-SE trending "Najd" shear zones was associated with intense igneous activity in Ediacaran time; these igneous rocks are especially abundant in Sinai and the NE Desert. Exposures along the E-W Nubian Swell from Aswan to Uweinat provide a glimpse of the transition from juvenile Neoproterozoic rocks of the Arabian-Nubian Shield westward into Archean and Paleoproterozoic rocks of the Saharan Metacraton. We have much to learn about the formation of Egypt's crust; the SE Desert is especially poorly known, and there are surprises to be discovered in the NE Desert basement. Future efforts to understand the crust of Egypt will require seismic refraction profiles to resolve its crustal structure; aeromagnetic mapping to resolve its crustal fabric; and drilling to sample basement buried beneath sediments of the vast Western Desert and Mediterranean coast.

R. J. Stern (✉)
Geosciences Department, The University of Texas at Dallas, Richardson, TX 75080, USA
e-mail: rjstern@utdallas.edu

K. Ali
Faculty of Earth Sciences, King Abdulaziz University, Jeddah, 21589, Saudi Arabia

Z. Hamimi et al. (eds.), *The Geology of Egypt*, Regional Geology Reviews,
https://doi.org/10.1007/978-3-030-15265-9_4

4.1 Introduction

Egypt is a large country, the 30th largest nation in area, covering over 1,000,000 km^2. Continental crust (also called "basement") underlies all of Egypt but is only exposed in ~10% of this area. Even though only a small fraction of Egypt exposes basement, these exposures span 800 km N-S and 1000 km E-W (Fig. 4.1). These extensive exposures provide a very useful if incomplete snapshot of Egypt's crust. Egyptian basement is exposed in 3 places: southern Sinai, the Eastern Desert, and in the southernmost Western Desert along the crest of the Nubian Swell.

In this chapter, the basement of Egypt is briefly summarized. These exposures can be subdivided into 5 smaller regions, from NE to SW: (1) Sinai; (2) Northeastern Desert; (3) Central Eastern Desert; (4) South Eastern Desert; and (5) Aswan and the Southwestern Desert subdivisions of the Eastern Desert are briefly reviewed. The first 4 subdivisions are dominated by Neoproterozoic rocks but the last subdivision contains basement of much greater age. In this chapter, we will conclude that the SE Desert and buried crust of the Western Desert are the new frontiers for future research. Our continuing dissection of Sinai strongly suggests that a similar level of effort in these two Eastern Desert terranes would resolve a similarly complex and interesting geologic history in these poorly studied regions.

Another important point is that our knowledge of Egyptian basement is incomplete, most importantly because most of it is hidden. Because ~90% of Egyptian crust is buried beneath sediments, we do not know whether or not the proportion of exposed basement is indicative of the buried crust. Future efforts to map this buried basement using geophysical techniques and sampling via drilling are needed to obtain a less-biased record of Egyptian crust, including both basement exposures and buried crust. Oil companies working in the Western Desert and N. Sinai may have such information. This chapter focuses only on exposed basement rocks.

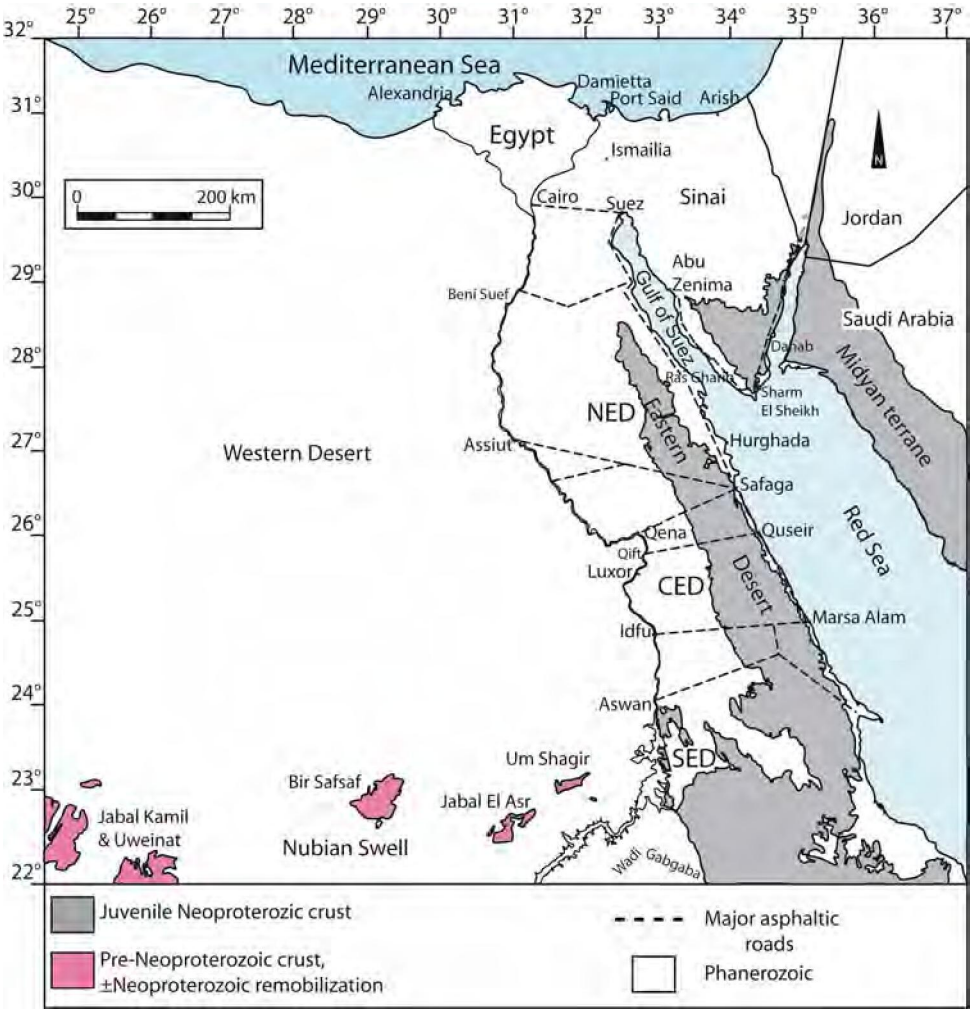

Fig. 4.1 Simplified geologic map of Egypt showing exposed Precambrian basement. NED = Northeastern Desert, CED = Central Eastern Desert, SED = Southeastern Desert

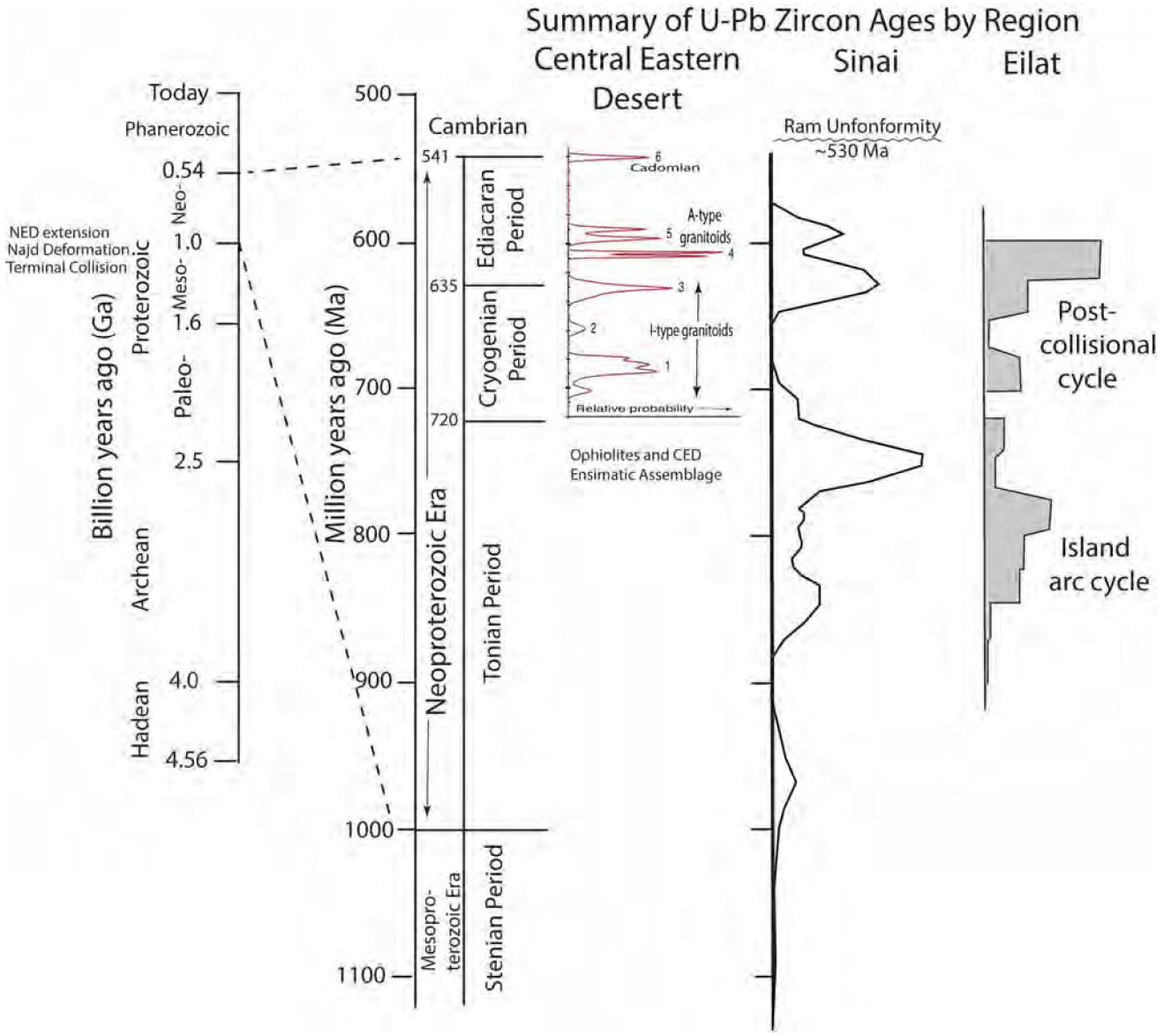

Fig. 4.2 Late Proterozoic temporal evolution of Egypt. Left: Geologic time, from Walker et al. 2012. Neoproterozoic time, showing time subdivisions used here. Also shown are the six magmatic pulses identified by Augland et al. (2012) for the Central Eastern Desert and relative crustal proportions as reflected by detrital zircons in Ediacaran terrestrial sediments (Samuel et al. 2011). The Rum unconformity—which signals cratonization of the ANS—is best exposed in Jordan and Israel but also eastern Sinai (Powell et al. 2014). This unconformity marks when the ANS—including the Eastern Desert—cooled and cratonized. "Cadomian" pulse ~540 Ma may be a far-field expression of Cadomian igneous activity as recently identified on the northern margin of the Arabian Plate (Stern et al. 2016a, b). Modified after Stern (2018) by adding summary curves for Sinai crust (Samuel et al. 2011) and exposures near Eilat (Morag et al. 2011)

When describing the basement of Egypt, it is essential to use the internationally-accepted subdivision of Precambrian time. This is shown in simplified form on the left side of Fig. 4.2, modified from Walker et al. (2012). The Neoproterozoic era is emphasized because the vast majority of exposed Egyptian basement rocks formed during this time period.

The crust of Egypt stabilized at the end of Ediacaran time. In general, stabilization of the crust follows cessation of igneous activity, which allows the crust to cool and strengthen. Further strength is gained from cooling and thickening of the underlying mantle lithosphere, which also happens after igneous activity stops. This strengthening of the continental crust and lithospheric mantle is often referred to as "cratonization". The great pulse of Neoproterozoic igneous activity in Egypt was over by ~580 Ma, although a minor "Cadomian" pulse occurred ~540 Ma (Augland et al. 2012). The clearest evidence of Egyptian cratonization is

cutting of the Rum Unconformity, which was completed by ~530 Ma. This unconformity is beautifully preserved in Jordan, Israel, and Saudi Arabia (Powell et al. 2014) but is only observed in Egypt in Sinai and in the far NE Desert. Elsewhere in Egypt, evidence of the Rum unconformity was obliterated by especially Cretaceous uplift, erosion, and deposition of the Nubian Sandstone.

4.2 Sinai

Precambrian basement in Sinai is exposed as a "V" with two arms, a short western arm extending NW along the eastern margin of the Gulf of Suez to ~29°N and a longer eastern arm extending to the border with Israel and beyond (Fig. 4.3). Sinai basement exposures encompass ~10,000 km^2 and consist of ~80% granite and ~20% volcanics and sediments (Stern and Hedge 1985). Exposed basement can be further subdivided into 3 groups, from oldest to youngest: (1) metamorphic complexes; (2) calc-alkaline; and (3) within-plate granitoids. Ediacaran rocks dominate over Cryogenian, Tonian, and Stenian rocks. These rocks are further discussed below.

The basement geology of Sinai can be simply described as islands of Tonian–Cryogenian metamorphic rocks floating in a sea of Ediacaran granites, all cut by Ediacaran dykes. From N to S, the four main metamorphic complexes exposed in Sinai are Taba, Sa'al, Feiran-Solaf, and Kid. Each of these metamorphic belts tells a different story about what existed in the region before the Ediacaran granite flood. Taba lies in the

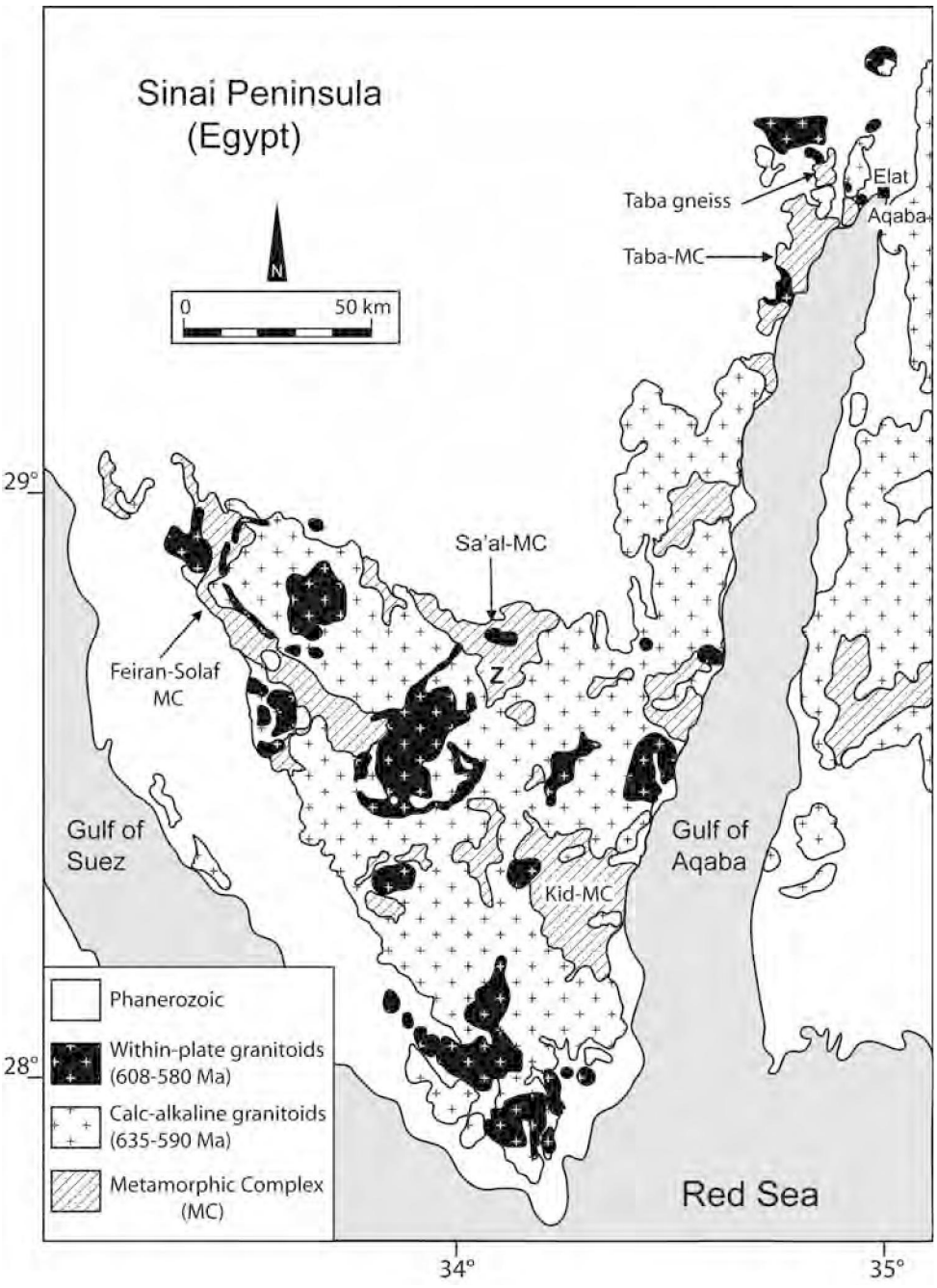

Fig. 4.3 Geological map of Sinai, showing the distribution of the main rock units and the main metamorphic complexes (MC) (after Eyal et al. 1980; Be'eri-Shlevin et al. 2009a, b). Z = location of Wadi Zaghra

far north, near the border with Israel. Basement exposures of the Taba complex extend for ~20 km along the northernmost western margin of the Gulf of Aqaba. This basement was uplifted associated with Late Neogene transtension along the Dead Sea Transform fault and broken up into the three small blocks, from S to N: Taba (Egypt), Elat, and Roded (Israel). Exposures of Tonian–Cryogenian metamorphic rocks are dominated by narrow E-W trending belts of metapelite separated by orthogneiss, all intruded by Ediacaran granites and dykes (Abu El-Enen et al. 2004). Amphibolite-facies metamorphism to ~640 °C and 6 kbar is documented (Abu El-Enen et al. 2004). Basement rock exposures in ED and Sinai are very similar to that exposed in the Elat Block and Roded Block in southernmost Israel (Morag et al. 2011). Basement exposures in this region preserve a remarkable variety of Neoproterozoic lithologies and ages (Abu El-Enen et al. 2004; Morag et al. 2011), in part because basement structure trends (E-W) are perpendicular to the uplift trend (N-S). Taba-Elat-Roded Complex metapelites contain detrital zircons dated at 800–820 Ma (Kröner et al. 1990) and its northern extensions in Israel (Elat Schist) and Jordan. More recent studies of metasediments near Elat (Elat association and Roded association) give detrital zircon ages of ~760 to ~850, with a few grains dating back to ~930 Ma (Morag et al. 2011). Dioritic to granitic orthogneisses intrude Elat complex metapelite and these intrusions are dated at 782–744 Ma (Kröner et al. 1990; Morag et al. 2011). Amphibolite bodies in the complex give ages of 670–612 Ma (Kröner et al. 1990; Morag et al. 2011). Similar rocks are also found in the Abu Barqa suite of SW Jordan, which has been displaced by ~80 km northwards due to Dead Sea Transform sinistral movements (Jarrar et al. 2013).

The Sa'al Metamorphic Complex in the north-central basement exposures of the Sinai peninsula provides a unique exposure of 1.12–0.95 Ga crust and sediments (Fig. 4.3) (Be'eri-Shlevin et al. 2012). This small belt strikes E-W and is dominated by two or three volcanosedimentary formations that were metamorphosed in greenschist to amphibolite facies (Eyal et al. 2014; Ali-Bik et al. 2017). Sa'al metavolcanics may have formed at a convergent plate margin (island arc). Crust of this age is recognized nowhere else in the Arabian-Nubian Shield. The influence of the ~1.0 Ga crust extends southward into Wadi Zaghra (Fig. 4.3) where deformed Ediacaran conglomerates (deposited ~615 Ma) contain ~1.0 Ga detritus as well as more abundant 750–850 Ma and 630–670 Ma detritus (Andresen et al. 2014). Sinai basement also preserves evidence of pre-Ediacaran crust near the Katherina complex where ~1.05 Ga inherited zircons are found in the 844 ± 4 Ma Moneiga quartz diorite (Bea et al. 2009).

The Feiran-Solaf Metamorphic Complex (Fig. 4.3) differs from Taba, Elat, and Sa'al complexes by covering a larger area (~100 km^2) and by having a strong NW-SE trending structure, 35 km long and 5–11 km wide (Fig. 4.3). Metamorphic rocks include ortho- and paragneisses and some calc-silicates, all flanked and intruded by granitic rocks. Its structure is dominated by a NW-trending anticlinorium cut by NW-trending thrust faults (Abu-Alam and Stüwe 2009). U-Pb zircon dating of Feiran-Solaf metamorphic complex rocks reveal a succession of magmatic and metamorphic events from ~1 Ga to <600 Ma (Abu El-Enen and Whitehouse 2013). Ages of ~1 Ga are found for zircons in meta-sandstones and from orthogneiss. Ages of 785–800 Ma are obtained from other orthogneisses (Abu El-Enen and Whitehouse 2013; Eyal et al. 2014). Metamorphism occurred between ~630 and ~590 Ma (Abu El-Enen and Whitehouse 2013). Abu-Alam and Stüwe (2009) concluded that Feiran-Solaf metamorphic rocks experienced peak metamorphism at ~700–750 °C and 7–8 kbar (~21.5–26 km deep in the crust) and subsequent isothermal decompression to ~4–5 kbar (~13–16.5 km deep in the crust). They argued that this was associated with shortening and concluded that ductile deformation associated with Najd shearing partly exhumed the gneisses during oblique transpression, but that the final ~15 km of exhumation happened later in Ediacaran time, perhaps associated with cutting of the Ediacaran unconformity ~600 Ma (associated with deposition of Hammamat and related sediments). An alternate tectonic interpretation, that the Feiran-Solaf metamorphic complex deformation reflects collision with the Sa'al Metamorphic Complex, is offered by Fowler et al. (in press).

The Kid complex is a volcano-sedimentary sequence occupying ~600 km^2 in southernmost Sinai (Fig. 4.3). It is similar to the other 3 metamorphic complexes in preserving pre-Ediacaran crustal remnants but differs in also preserving thick volcanic sections that formed at the beginning of the Ediacaran episode of igneous activity affecting Egypt. The Kid Metamorphic Complex consists of 4 major units: the mostly volcanic Heib and Tarr formations in the south and the volcaniclastic Melhaq and siliciclastic Um Zariq formations in the north, all separated by shear zones that formed at ~615–605 Ma (Moghazi et al. 2012). Qenaia migmatites and quartz diorite gneisses on the SW margin of the Kid complex, next to the Heib Formation, give a U-Pb zircon age ~768 ± 5 Ma (Eyal et al. 2014). The Heib, Tarr, and Melhaq formations reflect an intense episode of volcanism associated with Ediacaran core complex formation (Moghazi et al. 2012). The Heib Formation is a volcano-sedimentary succession and metarhyolites was dated by U-Pb zircon ages at 609 ± 5 Ma (Moghazi et al. 2012) and ~630–635 Ma (Eyal et al. 2014). The Um Zariq Formation consists of amphibolite-facies metapelites; detrital zircons give ages that mostly range between 895 and 730 Ma but a few are as young as ~647 Ma (Moghazi et al. 2012). Eyal et al. (2014) considered that these young ages reflect Pb-loss and that the Um Zariq Formation was deposited ~730 Ma.

Overall, the four metamorphic complexes of Sinai show evidence of having formed first as a 1000–700 Ma E-W belt that was disrupted in Early Ediacaran times by strong extension and exhumation in a marine environment (Azer et al. 2010) and followed by intense Najd shearing. The overall E-W trending fabric that defines Sinai and NE Desert crust was established in Stenian-Tonian time.

Calc-alkaline (CA) and alkaline-peralkaline (Alk) suites occupy ~80% of the Sinai basement exposures (Eyal et al. 2010). CA suite spans a wide range of mafic to felsic plutons (SiO_2 = 45–77 wt%). U-Pb zircon geochronology indicates prolonged and partially contemporary CA and Alk magmatism at 635–590 Ma and 608–580 Ma, respectively. Igneous rocks of the CA suite are further subdivided into deformed CA1 (650–625 Ma) and undeformed CA2 subsuites (Be'eri-Shlevin et al. 2009b). CA and Alk have distinct chemical compositions but mafic and felsic components have similar Nd, Sr, and O isotopic composition. Both suites have similar $\varepsilon_{Nd(t)}$ = +1.5 to +6.0 and indistinguishable, mantle-like mean zircon $\delta^{18}O$ = +5.8 and +5.9 (Be'eri-Shlevin et al. 2009a). Many have the characteristics of A-type granite. CA and Alk granitoids are probably related to mafic lower crust as inferred from analogous crust identified beneath western Arabia (Stern and Johnson 2010). Magmatic evolution of CA and Alk suites reflects mantle melting, mafic magmatism, and silicate melt fractionation into mafic lower and felsic upper crust. Distinct mantle sources are envisioned for CA and Alk suites, metasomatized lithospheric mantle for the former, upwelling asthenosphere due to delamination for the latter (Avigad and Gvirtzman 2009). Alk suites are associated with dense NE-trending dike swarms. These dike swarms are regionally bimodal and locally composite (Katzir et al. 2007), testifying to the coexistence of mafic and felsic magmas; similar dyke swarms are found in the NE Desert (Stern and Vogeli 1987; Stern et al. 1988). Volcanics also occur, especially in association with epizonal alkaline plutons (Azer et al. 2014).

It is worth noting that not all of the granitic intrusions in Sinai are part of the huge Ediacaran episode. There are also Tonian intrusions such as 782 ± 7 Ma El Sheikh granodiorite on the east flank of the Feiran-Solaf Complex (Stern and Manton 1987) and the 844 ± 4 Ma Moneiga quartz diorite along the southern extension of Feiran-Solaf, adjacent to the Katherina Ring Complex (Bea et al. 2009). These older plutons do not stand out in the field, and more likely await discovery in the Sinai basement. A similar conclusion that there is a significant proportion of pre-Ediacaran crust in the Sinai was reached on the basis of the abundant detritus in Ediacaran conglomerates (Samuel et al. 2011; Andresen et al. 2014).

Finally, remnants of Ediacaran terrigenous volcano-sedimentary successions are locally preserved in the Sinai basement. A good example is the ~620–590 Ma Rutig succession near Gebel Katherina. This is >2 km thick sequence of intermediate to felsic lavas and pyroclastics along with sandstones and conglomerates (Samuel et al. 2011). The Elat conglomerate is similar but may be younger (~580 Ma; Morag et al. 2012). These rocks reveal the Sinai in Ediacaran time as a magmatically active rift, with several terrestrial basins with rivers winding through desolate lava plains. An intriguing insight into what might lie at depth beneath northern Sinai and Egypt is provided by the Zenafim formation in the subsurface of Israel, which has been sampled by 4 drillholes along a ~150 km N-S transect (Avigad et al. 2015). This seems to mark an Ediacaran passive margin on the north side of Africa. The Zenafim formation thickens northward from thin alluvial fans in the south to >2 km thick marine sediments in the north; these sedimentary rocks testify to the encroachment of the proto-Tethys onto the margins of the subsiding Neoproterozoic orogen. U-Pb dating of detrital zircons from the alluvial fan facies reveal a concentration of 0.6–0.7 Ga ages, with a peak ~0.63 Ga; there is little evidence of older crust in these sediments (Avigad et al. 2015). In contrast, the marine facies is younger, ~0.58 Ga and contains abundant evidence of older crust.

4.3 Eastern Desert

Basement exposures in Egypt east of the Nile are found in the Eastern Desert (Fig. 4.4). These exposures encompass ~60,000 km^2 and reflect rift-flank uplift on the NW margin of the Red Sea. These can be subdivided along strike into Northeastern Desert (NED), Central Eastern Desert (CED) and Southeastern Desert (SED). These are discussed in this order below.

4.3.1 The North Eastern Desert

The NED lies north of a NE-trending boundary drawn south of the Qena-Safaga road and is the smallest (~10,000 km^2) of the three ED subdivisons. Like the Sinai, exposed NED crust is dominated by Ediacaran igneous rocks and associated sediments (Fig. 4.5). NED basement exposures are ~75% granite and gneiss and ~25% volcanics and sediments (Stern and Hedge 1985). Also similar to the geology of Sinai, there is strong evidence for extension in the form of abundant ~600 Ma bimodal dike swarms (including composite dikes) that trend E-W to NE-SW, indicating ~N-S oriented extension about the same time that Najd strike-slip deformation was affecting the CED (Stern et al. 1984). Abundant epizonal A-type granites require passive emplacement and indirectly demonstrate strong extension. The Ediacaran development of NED crust thus is very similar to that of Sinai, leading Stern et al.

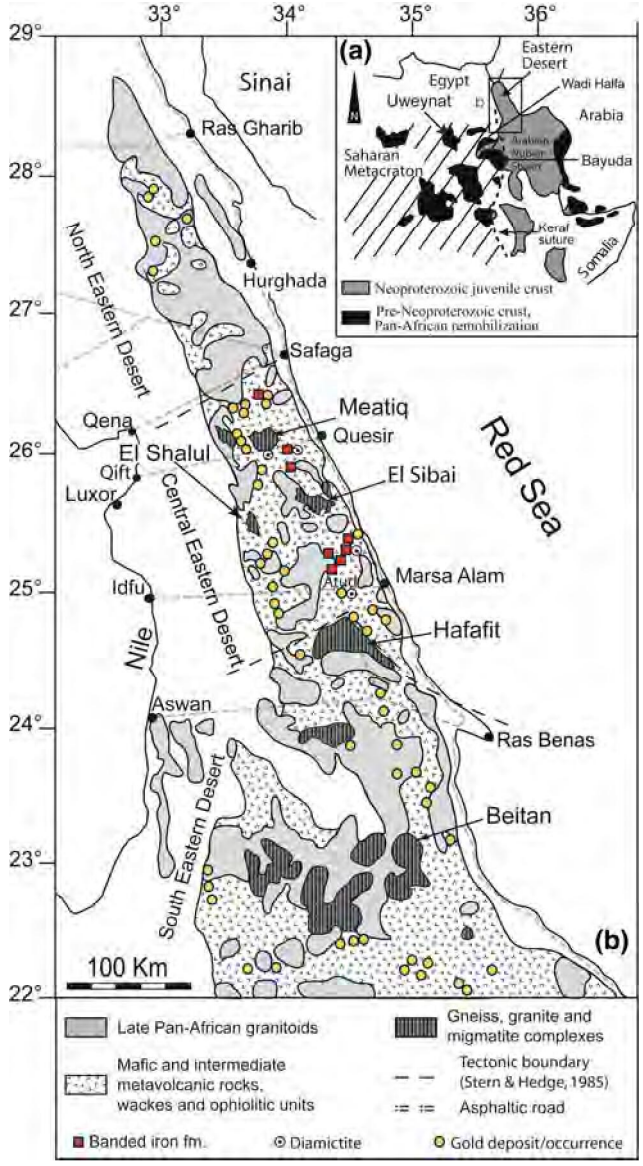

Fig. 4.4 **a**, *inset* Geological sketch map of NE Africa showing the Arabian-Nubian Shield, the Saharan Metacraton, and Archaean and Palaeoproterozoic crust that was remobilized during the Neoproterozoic. **b** Simplified geological map of the Eastern Desert of Egypt (modified from Stern and Hedge 1985) showing the BIF-diamictite sequences and gold deposits occurrences

(1984) and Stern (1985) to identify this region as the site of major NW-SE directed extension during Ediacaran time.

The geology of the NED is very different than the terranes to the south, especially the CED to its immediate south. The well-developed Cryogenian and Late Tonian sequences that are spectacularly exposed in the CED are missing. Ophiolites are absent and gneisses are rare. Distinctive Late Tonian–Ediacaran sediments especially banded iron formation (BIF) and Atud diamictite (Fig. 4.4b) are unknown from the NED (ophioites, BIF, and Atud diamictite are also missing from the Sinai). Evidence for Najd deformation—which affects the CED as well as western Arabia—is also missing. The Dokhan Volcanics were erupted during the Ediacaran "magmatic flare-up" (Stern and Hedge 1985; Wilde and Youssef 2000). There is disagreement as to whether Dokhan volcanism was associated with a continental arc or magmatic rift (Stern et al. 1984; Eliwa et al. 2006). It was thought up to recently that the overwhelming majority of NE Desert igneous rocks and associated Hammamat sediments were ~600 Ma, but recent investigations show that it is not quite this simple. Breitkreuz et al. (2010) reported U-Pb zircon SHRIMP ages for 10 Dokhan silica-rich ignimbrites and two subvolcanic dacitic bodies from the NED. These ages range between 592 and 630 Ma, indicating that Dokhan volcanism occurred over a 40 M.y. timespan.

In spite of the fact that NED and Sinai share a similar Ediacaran magmatic history, the NED contrasts with Sinai in having fewer documented examples of Cryogenian and Tonian crust. One of the most exciting recent developments in studies of the NED is that we are starting to identify small tracts of pre-Ediacaran crust. There have been hints of pre-Ediacaran crustal remnants in the NED for some time. One is the 666 Ma Mons Claudianus granodiorite (Stern and Hedge 1985); the 652 ± 3 Ma Um Taghir granodiorite collected along the Qena-Safaga road (Moussa et al. 2008) may be part of the Mons Claudianus batholith. Another is from SW of Gebel Dara near 27°50′N where Abdel-Rahman and Doig (1987) used whole-rock Rb-Sr geochronology to identify a Tonian muscovite tonalite. This is by far the oldest age reported for rocks of the NED and has yet to be confirmed by U-Pb zircon dating. Eliwa et al. (2014) used SIMS U-Pb zircon techniques to document the presence of ~740 Ma muscovite trondhjemite and ~720 Ma granodiorite from this area. Larger tracts of Tonian crust have recently been identified in the far NE Desert around 27°53′N where Bühler et al. (2014) studied the ~550 m thick Wadi Malaak succession of lavas, volcaniclastics, and clastic sedimentary rocks and documented the presence of ~720 Ma ignimbrites unconformably overlying ~740 Ma granitoids. Working in this general region but 15 km to the ESE, Abd El-Rahman et al. (2017) documented ~780 Ma dacite associated with Cu mineralization. Further efforts to identify and study slivers of Cryogenian–Tonian crust hidden in the NED are called for.

Ediacaran granitic rocks in the NED show remarkable mantle-like isotopic characteristics. Ali et al. (2016) studied 4 examples of these intrusions: the 653 Ma Um Taghir granodiorite, the 595 Ma Abu Harba intrusion, the 605 Ma Gattar syenogranite, and the 597 Ma Missikat syenogranite. All of these intrusions show strongly positive whole rock εNd(t) and zircon εHf(t), and zircon $\delta^{18}O$ ~ +3.6 to 6.7 per mill. The origin of the large volumes of enriched granite with such mantle-like isotopic compositions remains a mystery.

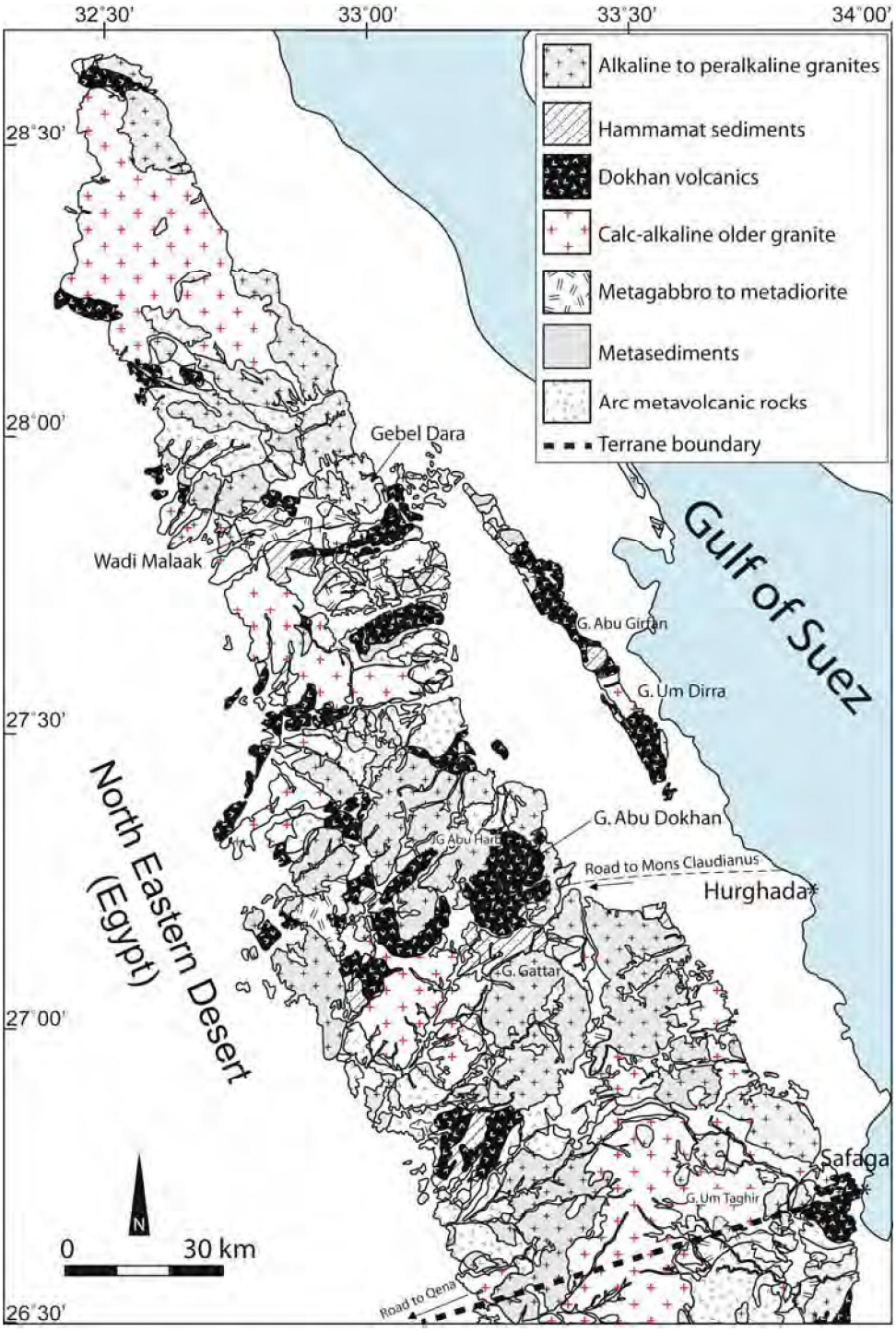

Fig. 4.5 Geological map for the North Eastern Desert of Egypt showing the Neoproterozoic basement rocks (modified from CONOCO map 1:500 000 and compiled from three quadrangle maps: Quseir quadrangle NG 36NE, Assuit quadrangle NG 36NW and Beni Suef quadrangle NH 36SW). General Petroleum Corporation, 1987, editors: Eberhard Klitzsch, Frank List, Gerhard Pöhlmann and associate editors: Robert Handley, Maurice Hermina and Bernard Meisner

4.3.2 The Central Eastern Desert

The CED lies south of the NED and north of an irregular boundary ~24°30′N where the SED begins (Fig. 4.6). CED exposures cover ~20,000 km^2 and consist of ~40% granite and gneiss, 55% sediments and volcanics, and ~5% serpentinites and related rocks (Stern and Hedge 1985). Much of the following information about the CED is adapted from Stern (2018). The CED best preserves the oldest (Tonian–Cryogenian) history of Egypt and also preserves Ediacaran deformation (Najd), volcanism (Dokhan) and sedimentation (Hammamat), all associated with intense igneous activity. The CED is by far the best known of the three Eastern Desert subdivisions. This is partly due to its

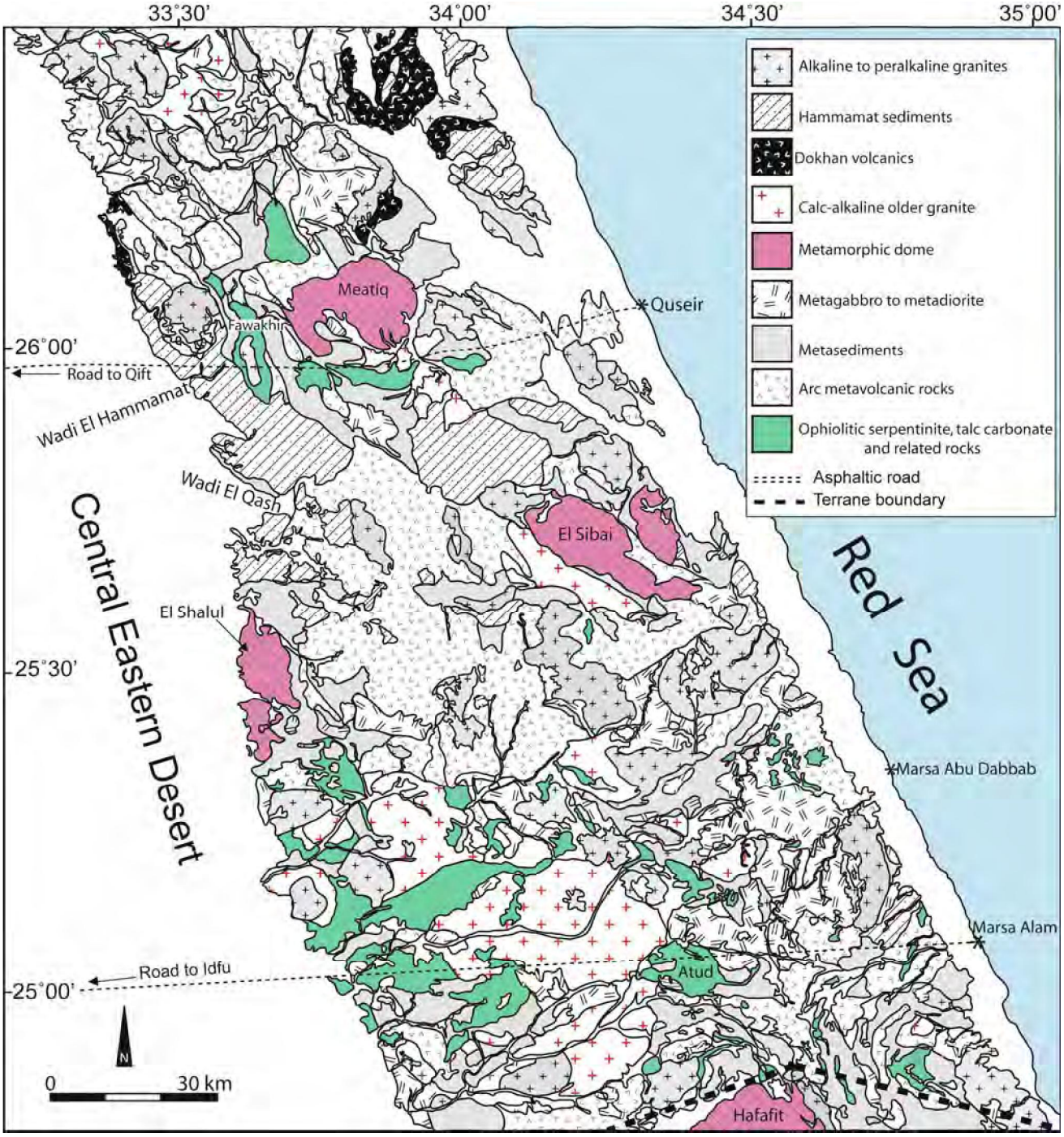

Fig. 4.6 Geological map for the Central Eastern Desert of Egypt showing the Neoproterozoic basement rocks (modified from CONOCO map 1:500 000 and compiled from two quadrangle maps: Quseir quadrangle NG 36 NE and Gabal Hamata quadrangle NG 36 SE). General Petroleum Corporation, 1987, editors: Eberhard Klitzsch, Frank List, Gerhard Pöhlmann and associate editors: Robert Handley, Maurice Hermina and Bernard Meisner

accessibility (it is traversed by two asphalt highways) and because it is a region of relatively subdued relief, but also because its supracrustal sequences are especially interesting and informative and because gold mineralization is concentrated here (Fig. 4.4).

The northern limit of the CED is a diffuse boundary marked by intrusions of granitic plutons of the southern NED. This transition is marked by a metamorphic gradient that increases northwards—from greenschist to amphibolite facies as the NED batholith is approached. It is more of a

broad transition zone than a sharp boundary and lies south of the Qena-Safaga road. The NED-CED transition zone has not yet been studied in any detail but may mark where the infrastructure-superstructure boundary intersects the surface. This transition is worthy of future research, including the extent to which it is metamorphic or structural (Qena-Safaga Shear Zone of Hamimi et al. 2019).

CED supracrustal sequences comprise an ensimatic (oceanic) assemblage characterized by a wide range of mostly greenschist-facies ophiolitic rocks and arc volcanics, along with volcaniclastic wackes, banded iron formation (BIF), and diamictite (Fig. 4.4b). The ensimatic assemblage comprises the oldest documented CED units, with ~750 Ma U-Pb zircon ages (Kröner et al. 1992; Andresen et al. 2009; Ali et al. 2009). The supercrustal ensimatic assemblage is punctured by Cryogenian I-type granitoids and Ediacaran I- and A-type granites (Fig. 4.6) and are further disrupted by several Ediacaran magmatic-metamorphic core complexes. These core complexes are locations where infracrustal "Tier 1" of Bennett and Mosely 1987) poke through lower-grade rocks of the superstructure ("Tier 2" of Bennett and Mosely 1987). CED supercrustal sequences are locally overlain by Ediacaran (~600 Ma) successor basins of the Hammamat Group. Hammamat basins formed in response to differential relief between higher regions in the NED and lower regions in the CED that accompanied Najd deformation in the CED and magmatic rifting in the NED. Possible links by one or more rivers between Ediacaran terrigeneous sediments in Jordan, Israel, Sinai, NED, and Hammamat sedimentary basins in the northern part of the CED warrant future focused investigations.

Eastern Desert infrastructure consists of upper amphibolite-facies quartzofeldspathic (granitic) gneisses and amphibolites exposed in several places in the CED, including the Meatiq, Abu Had, El Shalul, and El Sibai domes as well as the Migif-Hafafit and Beitan domes in the SED. These gneisses are intruded by dioritic, granodioritic, and granitic plutons, which formed in the infrastructure and differentially rose up through weak crustal shear zones. Infrastructure gneisses and intrusives are often mistakenly thought to be pre-Neoproterozoic "fundamental basement" but these clearly represent juvenile middle crust that formed in Neoproterozoic time, as shown by repeated radiometric and isotopic investigations (Liégeois and Stern 2010). The contact between superstructure and infrastructure is sometimes an intrusive contact and sometimes a high-strain mylonitic zone (see Stern 2018 for further details).

The CED is well known for its ophiolites, which comprise the base of the superstructure. We have two ages for CED ophiolites: (1) zircon evaporation $^{207}Pb/^{206}Pb$ ages of 745 ± 23 Ma for plagiogranite of the Wadi Ghadir ophiolite (Kröner et al. 1992) and U-Pb zircon TIMS age of 736.5 ± 1.2 Ma for gabbro from the Fawakhir ophiolite (Andresen et al. 2009). CED ophiolites are mostly highly disrupted and carbonated, although complete if abbreviated sequences of peridotites, gabbros, and pillow basalts are broadly exposed throughout the CED, for example along the Qena-Quseir road near Fawakhir and at Wadi Ghadir. Abdel-Karim and Ahmed (2010) summarized what is known about 38 different ophiolitic occurrences in the CED and SED. The volcanic section of these ophiolitic occurrences shows clear evidence of forming over a subduction zone, although it is controversial whether these formed in a backarc basin or in a forearc during subduction initiation (Abd El-Rahman et al. 2009a, b; Farahat 2010; El Bahariya 2018).

Understanding the significance of Eastern Desert ophiolitic ultramafic rocks is complicated because these are intensely altered by carbonate and sheared (Boskabadi et al. 2016; Hamimi et al. 2019). It is controversial how many episodes of deformation occurred but it is clear that ~600 Ma Najd deformation strongly affected the CED (Abdeen and Greiling 2005). Serpentinites and related talc-carbonates are weak, easily deformed and serve to localize major faults and shear zones. As a result, they form mélange that is easily mylonitized; some of carbonated ultramafics are so intensely sheared as to appear in the field to be bedded metasediments. Fortunately, modern orbital remote sensing technology allows us to identify the distinct spectral characteristics of serpentinite and carbonate from space (Sultan et al. 1986). Studies of CED ophiolitic ultramafics show that, before serpentinization and carbonation, these were highly depleted harzburgites (Azer and Stern 2007; Khalil and Azer 2007); such depleted peridotites are only found in forearc environments today.

Sedimentary rocks are important supracrustal components of the CED above the ophiolites. These are thick sequences of greenschist-facies arc volcanics and associated wackes and volcaniclastics. Early ideas that CED arc volcanic sequences stratigraphically overlie ophiolites and metasediments (Stern 1981) are not supported by U-Pb zircon geochronology. No discernible difference in age is found for ophiolites and arc sequences; both range from ~730 to ~750 Ma. One of the most interesting features of CED arc metavolcanics is that they sometimes contain abundant pre-Neoproterozoic zircon; these are especially common in mafic lavas (Ali et al. 2009; Stern et al. 2010a, b). These volcanics have mantle-like whole-rock Nd isotopic compositions and show no isotopic evidence for involvement of pre-Neoproterozoic crust, suggesting that the old zircons were inherited from the mantle (Stern et al. 2010a, b).

Metasediments occupy a significant proportion of CED outcrops. These are dominated by immature clastic sediments such as greywacke, siltstone and shale; many contain volcaniclastics and sometimes are interbedded with lava flows. These metasediments are broadly andesitic in bulk composition, but not much more is known about them. Future efforts to extract detrital zircon ages from

metawackes should provide useful insights into the geologic history of the CED.

Banded Iron Formation (BIF) and Atud diamictite are minor but very interesting components of the CED metasedimentary sequence (Fig. 4.4b). Atud diamictite is a poorly sorted, polymictic breccia, with clasts up to 1 m of granitoid, quartz porphyry, basalt, quartzite, greywacke, marble, arkose, and microconglomerate in fine-grained matrix (Ali et al. 2010a). The Atud diamictite is only documented from the CED, although a correlative unit, the Nuwaybah diamictite, is found in coastal Saudi Arabia (Ali et al. 2010a). Ali et al. (2010a) dated zircons from eight Atud diamictite clasts (five granitoids, 1 quartzite, 1 quartz porphyry, and 1 arkose) and a sample of diamictite matrix. The clasts gave a variety of ages. Two granitic clasts contained only Neoproterozoic (~750 Ma) zircons; another granitoid clast yielded mostly Neoproterozoic (0.75–0.79 Ga) zircons along with abundant 2.1–2.4 Ga zircons; a fourth granitoid also yielded Paleoproterozoic (2.0 Ga) ages, which were partially reset in Neoproterozoic time; the fifth granitic clast yielded only Paleoproterozoic–Archean ages. The quartz porphyry clast yielded mostly Neoproterozoic ages (697–778 Ma) along with one Early Paleoproterozoic and one Archean zircon. The quartzite clast yielded Paleoproterozoic to Archean (2.1–2.7 Ga) zircons. The arkose clast contained Neoproterozoic (0.72–0.77 Ga) and older Paleoproterozoic zircons (1.8–2.5 Ga). The diamictite matrix contains zircons with mixed Neoproterozoic and Paleoproterozoic ages (Ali et al. 2010a). There are no reliable pre-Neoproterozoic radiometric ages for in situ units in the CED or anywhere else in the Eastern Desert, so Atud diamicite pre-Neoproterozoic clasts and matrix components must have been derived from outside the CED and deposited in the oceanic basin that existed ~750 Ma in the CED. Ali et al. (2010a) inferred that Atud diamictite components may have been glacially eroded from the Saharan Metacraton to the west (Abdelsalam et al. 2002), where pre-Neoproterozoic and Neoproterozoic crust are both abundant (Sultan et al. 1994) during the Sturtian (~730 Ma) "Snowball Earth" episode.

Banded Iron Formation (BIF) is another diagnostic component of the CED metasedimentary sequence (Sims and James 1984; El-Shazly and Khalil 2014). There are thirteen different BIF localities in the CED (Fig. 4.4b). There is a correlative BIF occurrence in NW Saudi Arabia, the Sawawin deposit (Stern et al. 2013). Limited age constraints suggest that these BIFs formed ~750 Ma. CED BIFs consist of interlayered dense magnetite and hematite layers alternating with jasper. BIFs and interbedded wackes are strongly deformed and metamorphosed to greenschist and occasionally amphibolite facies. CED BIFs are related to distal submarine igneous activity and may reflect re-oxygenation of the ocean during or after the Sturtian glaciation (Stern et al. 2013).

The above overview indicates that the CED ~730–750 Ma was an ensimatic basin with an oceanic crustal structure. By analogy with modern oceanic crust, this would have been ~6 km thick. CED crust at this time may have been somewhat thicker because of associated arc volcanics and sediments. It is not clear when and how this region attained its present thickness of ~30 km (Hosny and Nyblade 2016). Some insight comes from the distribution of ~600 Ma Hammamat sediments, which define terrestrial basins that are especially well-developed in the northern CED, adjacent to the NED. These sediments were deposited on top of the Cryogenian sequences above an angular unconformity. Thicknesses of these sequences can reach several thousand meters (Fowler and Osman 2013). The Hammamat basins show that the much of the northern CED was low relative to the NED in Ediacaran time (Fowler and Osman 2013). Hammamat basins are filled with coarse clastic sediment that was largely eroded from the NED and carried by one or more rivers south and deposited in terrestrial basins that are now best preserved in the northern CED. The course of the Ediacaran river can be traced along the western flank of the Meatiq Dome (strongly deformed conglomerates of Wadi Um Esh; Ries et al. 1983) which opens up southward into a broad expanse of Hammamat NW of Wadis Hammamat, El Qash, and Arak (Fowler and Osman 2013). The crust that supported Hammamat Basins was somewhat above sea-level and so must have reached approximately its present thickness by that time. Hammamat basins formed in the CED formed without any evidence of Najd shearing and about the same time as Dokhan volcanism and intrusion of pink A-type granites, ~600 Ma. Fowler and Osman (2013) concluded that Hammamat sequences were deposited in basins formed by N-S extension.

Ediacaran granitic bodies were intruded in the CED but these are significantly less abundant than in the NED or Sinai. Early Ediacaran granitic rocks are mostly I-type whereas Late Ediacaran intrusions are mostly A-type (Fig. 4.2). There are also Cryogenian intrusions in the CED, although these are more poorly known.

There are significant gold deposits in the CED (Fig. 4.4b), including volcanogenic massive sulphide (VMS) deposits like Wadi Hamama (Abd El-Rahman et al. 2015) and gold mineralized quartz veins like El-Sid (Helmy and Zoheir 2015).

The southern limit of the CED is a sharp, structural boundary that follows the northern flank of the Migif-Hafafit dome (Shalaby 2010) and its continuation to the SW and SE. The Migif-Hafafit complex represents an excellent window into the infrastructure-superstructure transition and the nature of the infrastructure, which repeated geochronologic and isotopic measurements indicate is a juvenile Neoproterozoic crustal addition (Liégeois and Stern 2010). The boundary is a complex fault system that can be traced for several tens of kilometers NW along Wadi Nugrus and Gebel Hafafit, then

turns abruptly SW along Gebel Migif and Wadi Shait to mark the boundary between superstructure and the CED to the north and infrastructure and the SED to the south.

4.3.3 The South Eastern Desert

Precambrian basement exposed in the SED covers a much larger area (~30,000 km^2) and is much less studied than the basement exposures of Sinai, the NED or the CED. In many ways, the SED represents the "last frontier" for future studies of the Precambrian basement of Egypt; this reflects its remote location and lack of asphalt roads.

The SED can be partially defined by its geologic boundaries (Fig. 4.7). In the north is the mostly tectonic boundary with the CED, described in the previous section. The eastern boundary is defined by the Red Sea coastal plain. Before the Red Sea opened in mid-Cenozoic time, the SED was contiguous with the Midyan terrane of NW Arabia (Johnson and Woldhaimanot 2003), which is also poorly known. The southern boundary of the SED is marked by the Nubian portion of the Yanbu-Sol Hamed-Onib-Gerf-Allaqi-Heiani (YOSHGAH) suture; Stern et al. 1990). The western boundary is poorly defined but seems to trend ~N-S along ~33°E just east of the Nile, where abundant Ediacaran granitic rocks outcrop discontinuously around Aswan and farther south; these have Nd isotopic compositions and inherited zircons that indicate involvement of older crust (Sultan et al. 1990; Finger et al. 2008).

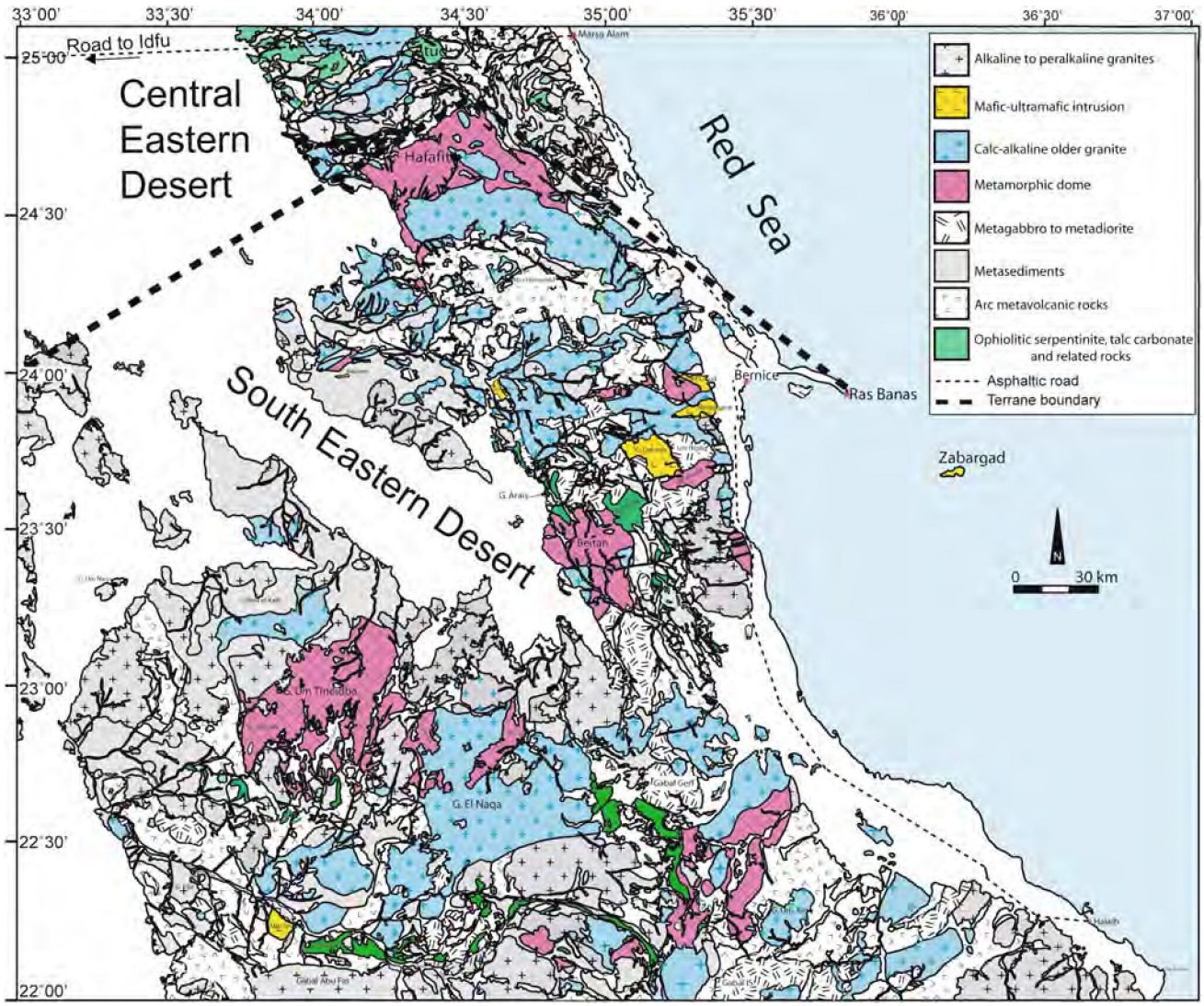

Fig. 4.7 Geological map for the Southern Eastern Desert of Egypt showing the Neoproterozoic basement rocks (modified from CONOCO map 1:500 000 and compiled from two quadrangle maps: Gabal Hamata quadrangle NG 36 SE and Bernice quadrangle NF 36 NE). General Petroleum Corporation, 1987, editors: Eberhard Klitzsch, Frank List, Gerhard Pöhlmann and associate editors: Robert Handley, Maurice Hermina and Bernard Meisner

The SED contrasts with the CED by lacking BIF deposits. It may also lack possible glaciogenic deposits comparable to the Atud diamictite, although these have not been actively searched for. The SED also lacks significant Ediacaran sedimentary or volcanic successions such as the Hammamat Group and Dokhan Volcanics found in the NED and CED, although SED volcanic successions have been mistakenly assigned to the Dokhan. The SED and CED contain similar proportions of serpentinites but these are scarcely studied except for ophiolites along the E-W trending Allaqi-Heiani-Gerf suture in the far south SED YOSHGAH suture and at Abu Dahr (Gahlan et al. 2015). The SED seems to also show infrastructure-superstructure relationships like those of the CED, but the units in the SED are somewhat older (Stern 2018). The SED in general seems to represent a deeper level of exposure than the CED and is much less affected by Najd shearing. Because the SED is less studied than the CED, there is less geochronologic data; what is available suggests that it is generally slightly older than the CED (Stern and Hedge 1985), but more geochronological studies are needed in order to better outline the main features of SED crust.

The northernmost SED is dominated by gneiss, migmatite, and granitic rocks of the Migif-Hafafit region, a belt that trends ~E-W. This complex metamorphic dome represents an unusually large exposure of infrastructure (Bennett and Mosely 1987) and is separated from the southernmost CED by a broad mylonitic shear zone, the Nugrus thrust. Gneissic metagabbros define large scale fold interference patterns cored by foliated meta-tonalites (Fowler and El Kalioubi 2002). Three of these intrusions give zircon Pb evaporation ages of 675–700 Ma (Kröner et al. 1994) and have Nd and Sr isotopic compositions indicating that these are juvenile crustal additions (Liégeois and Stern 2010).

South of the Migif-Hafafit gneissic terrane is a large and poorly known granitic batholith. South of the great, poorly studied E-W trending batholith there is a great E-W volcanic belt ~25 km wide, the Shadli metavolcanics. This name is sometimes mistakenly applied to CED metavolcanic rocks but the two sequences are different. Near the Umm Samiuki mine, the Shadli metavolcanics consist of the older Um Samiuki and the younger Hamamid groups, both comprising mafic to felsic successions of slightly metamorphosed lavas. They both comprise bimodal suites with modes at 48–53 and 69–75 wt% SiO_2. Basalts can be further subdivided into a fractionated low K, high-Ti (~0.3 wt% K_2O; >2 wt% TiO_2) and a primitive med.- K, low-Ti (~1 wt% K_2O; ~1 wt% TiO_2) suites. These are both fairly depleted suites, with flat or LREE-depleted REE patterns (Stern et al. 1991). A composite Rb-Sr whole rock isochron age of 711 ± 24 Ma and $\varepsilon Nd(t)$ = +6.3 to +7.8 was also reported by Stern et al. (1991); U-Pb zircon ages for these volcanics are needed. On trace element discrimination diagrams, these volcanics plot outside the field of arc lavas; formation in a magmatic rift was suggested by Stern et al. (1991). This metavolcanic belt is associated with polymetallic massive Zn-Cu-Pb-Ag sulfides, such as El Atshan, Egat, Derhib, Abu Gurdi, Helgate, Maqaal, and Um Samiuki (Helmy 1999). These deposits probably reflect submarine hydrothermal deposits.

On the southern margin of the Shadli metavolcanic belt there are several mafic-ultramafic Alaska-type and layered intrusions aligned ~E-W around 24°N. From W to E these are: (1) Gabbro Akarem (24°00′N, 34°08′E, ~12 km^2); (2) Gabbro Gharbia (23°56′N, 34°38′E ~12 km^2); (3) Abu Hamamid (24°19.5′N, 34°44′E, ~0.5 km^2); Dahanib (23°46′N, 35°10′E, ~9 km^2); El Motaghairat (23°52′N, 35°23′E, ~8 km^2); and Zabargad in the Red Sea (23°37′N, 36°11′E, ~7.5 km^2). We do not know if these are different manifestations of a single igneous event because we only have radiometric ages for a quartz diorite near Dahanib (U-Pb zircon age of 711 ± 7 Ma; Dixon 1981a, b), approximate Rb-Sr and Sm–Nd ages of 650–700 Ma for Zabargad peridotites (Brueckner et al. 1995), Sm–Nd errorchron of 963 ± 81 Ma for Genina Gharbia (Helmy et al. 2014).

Gabbro Akarem is a concentrically-zoned mafic-ultramafic intrusion (dunite core, then hornblende lherzolite, olivine–plagioclase hornblendite, and plagioclase hornblendite (Helmy and El Mahallawi 2003). It is elongated ~80°E–260°W, ~10 km long and ~2 km wide, intruded into metasediments. All lithologies have essentially flat REE patterns. Genina Gharbia is an elongated NW-SE (~3 × 6 km) cumulate intrusion into metasediments. It consists of a core of pyroxenite and peridotite surrounded by norite and gabbro (Helmy 2004), all with Nd isotopic compositions indicating derivation from depleted mantle. Abu Hamamid is elongated and intruded into Shadli volcanics (see below) on the north and granodiorite on the south (Helmy et al. 2015). It is zoned from dunite through clinopyroxenite to gabbro. A Sm–Nd isochron suggests an age of 963 ± 81 Ma (Helmy et al. 2014). Dahanib is a tilted layered intrusion oriented N-S, ~6 km × 2 km, composed of peridotite (dunite, wehrlite, lherzolite, pyroxenite, and gabbronorite/norite (Dixon 1981a, b; Azer et al. 2017). Trace elements of Dahanib igneous rocks indicate a convergent margin tectonic environment (Azer et al. 2017). El Motghairat consists of a NE-elongated ~4 × 1 km layered intrusion of basal dunite, lherzolite, and pyroxenite; dominant troctolite; and upper gabbro and anorthosite intruded into metagabbro (Abdel-Halim et al. 2016). The Zabargad intrusion consists of scattered exposures of amphibole-bearing plagioclase peridotites on a small (~3 km across) island (Agrinier et al. 1993). Zabargad peridotites are emplaced into HP-HT metamorphic rocks (850 °C, 10 kbar or ~33 km deep in the crust; Boudier et al. 1988) these gneisses give Rb-Sr and Sm–Nd ages of 655 ± 8 Ma and 699 ± 34 Ma, interpreted as dating peak metamorphism (Lancelot and Bosch 1991).

SED mafic-ultramafic intrusions are associated with potentially economic deposits of Cu-Ni-PGE (Helmy 2004). Gabbro Akarem and Genina complexes contain Cu-Ni-PGE ores, but these are currently deemed sub-economic (700,000 tons of ore at Gabbro Akarem with ~2 wt% Cu and Ni; Genina Gharbia contains hundreds of thousands of tons of ore with <1 ppm PGE).We have much to learn about the age and significance of these and similar deposits further south ~22°N at Abu Fas and Gerf-Khobani, most importantly whether they are the same age or not. Remote sensing studies would be useful for mapping these intrusions and to help search for more of these spectrally-distinctive bodies.

The region between the Shadli Metavolcanics ~24°30′N and the YOSHGAH suture near 22°N is especially poorly known. There are two key pieces of age information for this poorly-known region, both indicating an age of ~710–750 Ma. One is a U-Pb zircon age of 711 ± 7 Ma for a tonalite from Wadi Shut (23°45′N, 35°12′E; Dixon 1981b) and the is for hornblende-bearing orthogneisses along Wadi Beitan (~23°20′N, 35°E), where U-Pb zircon ages of 719 ± 10 Ma, 725 ± 9 Ma, and 744 ± 10 Ma are reported (Ali et al. 2015). Zircon εHf(t) values of −4.8 to +12.5 in the Beitan gneisses hint that pre-Neoproterozoic crustal remnants might exist in the SED although whole-rock εNd(t) values of +5.1 to +6.6 indicate this is an overwhelmingly juvenile crustal addition (Ali et al. 2015).

The southernmost geologic feature of interest in the SED is the Yanbu-Sol Hamed-Onib-Gerf-Allaqi-Heiani (YOSHGAH) suture. The YOSHGAH suture is decorated with abundant ophiolites and can be traced for ~600 km across SE Egypt, NE Sudan, and NW Saudi Arabia (Stern et al. 1990). The YOSHGAH suture in Egypt trends approximately E-W just N of the Egypt-Sudan border until it intersects the N-S trending Hamasana Shear Zone ~34°40′ E. YOSGAH ophiolites and surrounding rocks in the SED are studied in the east (Gerf; east of 35°E) and the west (Allaqi; west of 34°E), with few studies in between.

The Gerf complex is the largest ophiolite in Egypt (~1–5 km wide, ~17 km long) and consists of basaltic pillow lavas, sheeted dykes, isotropic and layered gabbros and ultramafic mélange, all in thrust contact. Zimmer et al. (1995) concluded from major and trace element data that pillow lavas and sheeted dykes are indistinguishable from modern high-Ti N-MORB whereas Abdel-Karim et al. (2016) concluded from analyses of peridotites and pyroxenites that Gerf formed in a fore-arc supra-subduction zone (SSZ) environment. Kröner et al. (1992) analyzed single zircons from a coarse leucogabbro within the layered sequence using the evaporation method. They obtained a mean $^{207}Pb/^{206}Pb$ age of 741 + 42 Ma (2σ error) for four grains and interpreted this as the crystallization age of the gabbro and thus the ophiolite. εNd(t) values of +6.5 to +7.9 indicate derivation from depleted mantle (Zimmer et al. 1995).

Within the Halaib area is found the northernmost part of the N-S Hamisana shear zone (HSZ) and the Onib segment of the YOSHGAH suture. The HSZ formed after collision formed the YOSHGAH suture and consists of amphibolite-facies meta-igneous and metasedimentary rocks intruded by deformed granitic plutons. The HSZ stands out because it trends N-S encompassing about 1500 km^2 of southeastern Egypt and northeastern Sudan and disrupts the older, ~E-W trending YOSHGAH. de Wall et al. (2001) used anisotropy of magnetic susceptibility along with field and microstructural studies to demonstrate that HSZ deformation was dominated by pure shear, producing E–W shortening with a strong N–S-extensional component. This deformation also led to folding of regional-scale thrusts (including the YOSHGAH ophiolite and related structures). Metamorphism to amphibolite facies (up to 600 ± 50 °C and 5–6.5 kbar, or 15–20 km deep in the crust; Ali-Bik et al. 2014). Three zircon Pb–Pb evaporation and two U-Pb conventional zircon ages range from 663 ± 29 Ma to 844 ± 10 Ma ± 5 Ma; Rb-Sr whole rock isochron and errorchron ages for 7 deformed granitic and gneissic bodies range from 551 ± 28 Ma to 665 ± 62 Ma; these ages reflect a protracted episode of Neoproterozoic crust formation and deformation. Two mineral isochrons and one undeformed granite give ages of 510 ± 40 Ma to 573 ± 15 Ma, indicating that exhumation and cooling encompassed a significant amount of Late Ediacaran and perhaps Cambrian time (Stern et al. 1989). The northern HSZ thus provides a remarkable exposure of exhumed ANS middle crust, worthy of further integrated study involving structural, metamorphic, and geochronological studies.

The western YOSHGAH suture has been studied around Wadi Allaqi west of 34°E. Abdelsalam et al. (2003) carried out structural studies supported by remote sensing to show that this part of the suture zone constitutes three S-to SW verging low-angle thrust sheets and folds, forming a 10 km wide imbrication fan. Similar conclusions were reached by Hamimi et al. (2019). Volcanic rocks including rhyolites and felsic tuffs above metasedimentary rocks dominate the upper allochthon. This overrides the central allochthon dominated by arc and ophiolitic assemblages. The structurally lowest nappe (southern allochthon) is dominated by amphibolite facies schistose metavolcanic and metavolcanoclastic rocks. Serpentinized ophiolitic peridotites are very depleted and interpreted as fragments of forearc mantle on the basis of major element and spinel compositions (Azer et al. 2013). Mafic to felsic metavolcanics mapped as Dokhan volcanics are exposed along Wadi Allaqi south of the southern allochthon (El-Nisr 1997).

There is some robust geochronological control for rocks around the Allaqi segment of YOSHGAH. Kröner et al. (1992) obtained single zircon Pb–Pb evaporation ages of 729 ± 17 Ma and 736 ± 11 Ma for gabbro and diorite

samples, respectively, from a single intrusion into sheared serpentinites; they were uncertain whether the dated gabbrodiorite was part of the ophiolite or intruded it, but finally interpreted it as a post-obduction intrusion. Ali et al. (2010b reported five SHRIMP U-Pb zircon ages. Ophiolitic layered gabbro gave a concordia age of 730 ± 6 Ma, and a metadacite from overlying arc-type metavolcanic rocks yielded a weighted mean $^{206}Pb/^{238}U$ age of 733 ± 7 Ma. Taken together—and considering the results of Kröner et al. (1992)—this indicates ophiolite formation at ~ 730 Ma. The Allaqi ophiolite is thus similar in age to Gerf and CED ophiolites. Ophiolite emplacement in Wadi Allaqi is constrained by U-Pb zircon concordia ages for intrusive gabbro (697 ± 5 Ma) and quartz diorite (709 ± 4 Ma) indicating <30 million years between ophiolite formation by seafloor spreading and terrane accretion.

4.4 Aswan and the Southwestern Desert

Crust of the Western Desert of Egypt (Fig. 4.8) is mostly buried beneath Phanerozoic sediments. Some oil companies have drilled to basement but information about the basement they encountered is not yet available to the public. Maps of the magnetic field over this huge region would also be useful for understanding basement lithologies and trends but these are not available as of this writing in early 2018. Fortunately, the Nubian Swell—an E-W trending uplift extending ~800 km to the border of Libya (Thurmond et al. 2004)—allows glimpses of this buried basement. We know that crust on the buried northern flank of Arabia is mostly younger than ANS crust and suspect that this is also true for adjacent parts of Egypt, but the E-W transect provided by Nubian Swell exposures are nevertheless extremely informative about the nature of Egyptian crust buried beneath the Western Desert.

It is not easy to define the boundary between juvenile Neoproterozoic crust of the Eastern Desert and older crust of the northwestern Saharan Metacraton in the Western Desert of Egypt. This is sometimes interpreted as a tectonic boundary, with Eastern Desert ensimatic assemblages thrust over the Metacraton (e.g., Hamimi et al. 2019), but the boundary is obscured by Ediacaran granitic intrusions. There are extensive outcrops of Archean and Paleoproterozoic rocks in the far west along the Nubian Swell around Gebel Kamil and Gebel Oweinat but farther east these disappear and are replaced by mostly Ediacaran igneous rocks that preserve isotopic evidence that pre-Neoproterozoic crust once existed here. Previous workers take the granitic exposures around Aswan to mark the boundary between the Saharan Metacraton and juvenile Neoproterozoic crust of the SED (Harris et al. 1984; Sultan et al. 1990). These exposures include several varieties of granite along with tonalite, pegmatite, and metamorphic rocks (Gindy and Tamish 1998). U-Pb zircon ages by TIMS and LA-ICP-MS give ages of 595 ± 11 Ma to 622 ± 11 Ma for Aswan plutonic rocks (Finger et al. 2008) and 634 ± 4 Ma for granitic gneiss from Aswan (Sultan et al. 1994). These granitic rocks show isotopic evidence for the involvement of pre-Neoproterozoic crust, especially in terms of whole rock εNd(t) = +1.0 to +2.3 (Harris et al. 1984; Sultan et al. 1990).

Basement exposures SW of Aswan and Gebel Umm Shagir are the next important basement exposures west of Aswan and the Nile. These outcrops are dominated by migmatite, gneiss, post-tectonic granite, dikes, and sills (Bernau et al. 1987; Sultan et al. 1994). Biotite granite gneiss from 160 km SW of Aswan along the road to Abu Simbel gave a U-Pb zircon TIMS age of 741 ± 5 Ma whereas a granitic migmatite from Gebel Umm Shaghir gave a U-Pb zircon TIMS age of 626 ± 4 Ma (Sultan et al. 1994).

The next important outcrop to the west of Gebel Umm Shaghir is around Gebel El Asr, where amphibolite- to granulite-facies quartzo-feldspathic gneiss and other metamorphic rocks (including BIF) dominate and intrusive rocks are subordinant (Bernau et al. 1987). Anorthosite from Gebel El Asr contain an unusually complex zircon population, with 2 fractions that give a TIMS U-Pb zircon concordia age of

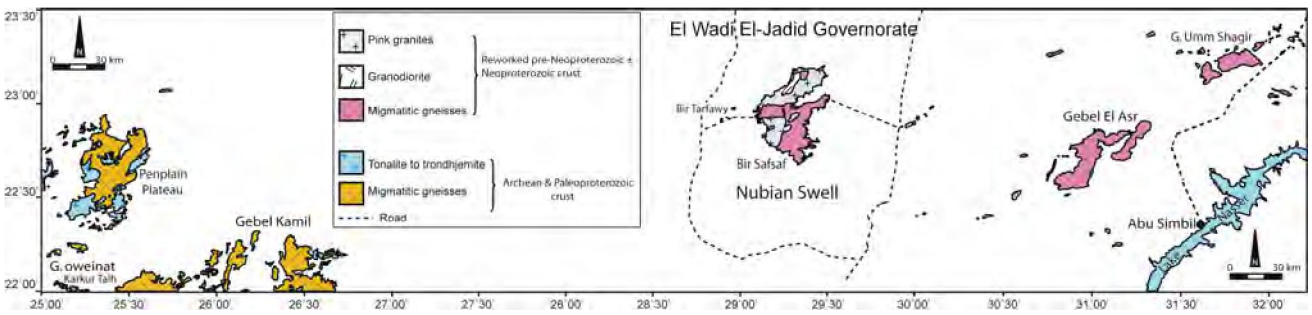

Fig. 4.8 Geological map for the Southern Western Desert of Egypt showing the pre-Neoproterozoic and Neoproterozoic remobilization basement rocks (modified from CONOCO map 1:500 000 and compiled from two quadrangle maps: Gilf Kebir Plateau quadrangle NF 35 NW, Bir Misaha quadrangle NF 35 NE and El-Saad El-Ali quadrangle NF 36 NW). General Petroleum Corporation, 1987, editors: Eberhard Klitzsch, Frank List, Gerhard Pöhlmann and associate editors: Robert Handley, Maurice Hermina and Bernard Meisner

604 ± 5 Ma and a discordia with a lower intercept age of ~689 Ma and upper intercepts of 1922–2141 Ma (Sultan et al. 1994). These ages give clear evidence that pre-Neoproterozoic crust was intensively reworked in Neoproterozoic time.

Bernau et al. (1987) identified three metamorphic stages for rocks of Gebel Umm Shaghir and Gebel El Asr. The first stage is reflected in scapolite formation in calc-silicates, indicating lower T limits of ~800 °C and P ~8–9 kb (~25–30 km deep in the crust). The second stage is shown by the breakdown of scapolite into anorthite and calcite and occurred at T ~750–800 °C and P < 6 kbar (<~20 km deep in the crust). The third stage was retrogression under greenschist-facies conditions. E-W trending mylonite zones are common in basement outcrops around Umm Shaghir and El Asr (Bernau et al. 1987).

The next major outcrop of basement to the west along the Nubian Swell is around Bir Safsaf. This is a very large exposure, encompassing ~1000 km^2. Bernau et al. (1987) show this large region as consisting of subequal proportions of metamorphic and plutonic rocks (granite and granodiorite), all cut by dikes, but Bea et al. (2011a) depict it as consisting entirely of various granitic rocks. Some of the granites contain muscovite and show affinities with S-type granites (Bernau et al. 1987). The dominant igneous rock at Bir Safsaf is coarse red biotite granite (Bernau et al. 1987) or pink granite, syenogranite, and granodiorite (Bea et al. 2011a); this intrudes granodiorite and sometimes contains abundant xenoliths of the older granodiorite (Bea et al. 2011a). Bea et al. (2011a) carried out U-Pb SHRIMP dating of zircons from 9 samples of Safsaf gneissic and granitic rocks. Their results indicate that all Safsaf granitoids and migmatitic gneisses formed during an Ediacaran magmatic event that lasted from 627 to 595 Ma. They also noted that some zircon cores and xenocrysts show ages of 2.1 and 2.7 Ga. They also analyzed 28 whole-rock samples for Sr isotopic compositions and found that these defined an errorchron with an age of ~616 Ma and an initial $^{87}Sr/^{86}Sr$ ~0.7050. Twenty-eight analyses of whole-rock Nd isotopic compositions yielded a narrow range of εNd(t), between −5 and −6, clearly indicating the presence of pre-Neoproterozoic crust. Bea et al. (2011a) obtained Nd model ages of ~1.5 Ga but interpreted this as having no age significance but as an artifact of mixing between 2.1 and 2.7 Ga old crust and juvenile Neoproterozoic melts.

Gebel Kamil is the next exposure to the west of Bir Safsaf. The area around Gebel Kamil is the easternmost part of the ~200 km wide basement outcrop that continues all the way to Gebel Oweinat at the border with Libya and Sudan, and here the oldest rocks in Egypt are exposed. Sultan et al. (1994) dated five grains from a gabbroic anorthosite from Gebel Kamil using TIMS U-Pb zircon techniques. Two single-grain analyses yielded identical $^{207}Pb/^{206}Pb$ ages of 2629 ± 3 Ma whereas three multigrain fractions and two single grains define a discordia with an upper intercept age of 2063 ± 8 Ma and a poorly defined Neoproterozoic lower intercept age. Sultan et al. (1994) interpreted these results as reflecting an Archean igneous rock that was metamorphosed in Paleoproterozoic time. Bea et al. (2011b) confirmed the presence of Archean crust in the Gebel Kamil—Gebel Oweinat uplift and a Paleoproterozoic (~2.1 Ga) overprint. Bea et al. (2011b) also documented a meta-igneous complex that they called the Gebel Kamil complex, composed of low- to medium-K calcic to calc-alkaline tonalitic to trondhjemitic, rarely granitic, gneisses (TTG) associated with subordinate gabbro-dioritic gneisses. These TTGs yield a Sm–Nd whole-rock isochron age of 3.16 ± 0.16 Ga and have a range of U-Pb zircon ages from 2.55 to 3.1 Ga. The most primitive TTG gneisses contain zircons with crystallization ages between 3.1 Ga and 3.3 Ga peaking at 3.22 ± 0.04 Ga, almost identical, within error, to the Sm–Nd isochron. These are by far the oldest rocks in Egypt and some of the oldest rocks in Africa.

Karmakar and Schenk (2015) studied textural and compositional relationships in metapelites and metabasites from all over the Gebel Kamil—Gebel Oweinat area. Metapelitic granulites show a two-stage metamorphic evolution; the first stage occurred at ~1050 °C and P ~10 kbar (~33 km deep in the crust), and the second stage involved near-isothermal decompression to ~6 kbar at T of 900–1000 °C followed by near-isobaric cooling to temperatures of ~700 °C at 5.5–6 kbar (17–20 km deep in the crust). Karmakar and Schenk (2015) also documented the second metamorphic stage in the associated metabasic granulites. Karmakar and Schenk (2015) conducted texturally-controlled in situ Th–U–total Pb monazite dating of the metapelites and concluded that metamorphism first occurred at ~2.6 Ga during an episode of Neoarchean ultrahigh-temperature metamorphism. The second stage occurred ~1.9 Ga during a Paleoproterozoic ultra-high temperature isothermal decompression event. Karmakar and Schenk (2015) found no evidence of significant Neoproterozoic metamorphism.

4.5 Buried Crust of the Western Desert

No summary of the Precambrian basement of Egypt would be complete without mention of crust buried beneath Phanerozoic sediments west of the Eastern Desert and north of the Nubian Swell. We know nothing about this crust. Aeromagnetic and gravity maps would be useful, but these

are not readily available. Oil and gas drilling in this vast region may have sampled this basement, but if so we know nothing about where these penetrations occurred or what was found. Nor can we extrapolate from the buried basement of Libya, this crust is also unknown. What we do know is that buried crust north of the Arabian Shield is surprisingly heterogeneous. We know that 1.2–0.95 Ga crust is exposed in Sinai. There is evidence of a Late Ediacaran (~580 Ma) passive margin developed on the NW flank of Arabia (Zenafim Formation; Avigad et al. 2015) buried beneath younger sediments in Israel, and a similar passive margin sequence might lie beneath the Phanerozoic sediments of the Western Desert. We also know that Cadomian crust ~560 Ma lies beneath sediments in northern Jordan (Stern et al. 2016a, b) and that Carboniferous crust ~357 Ma lies beneath sediments in southern Syria (Stern et al. 2014). It will be for the next generation to explore the buried crust of Egypt. Who knows what they will find?

4.6 Conclusions

Our overview of Egyptian basement rocks can be summarized in the following 10 points:

1. Only a small fraction (~10%) of Egyptian crust is exposed and available for study. Most of this exposed crust is Neoproterozoic in age.
2. Exposures around the Red Sea mark the NW extent of the Arabian-Nubian Shield. These are readily subdivided into 4 basement provinces: Sinai, NE Desert, Central E Desert, and SE Desert. Basement exposures from Aswan westwards along the Sudan border to the border with Libya represent a fifth basement province, the SW Desert.
3. Sinai basement exposures include small remnants of Cryogenian, Tonian, and Late Mesoproterozoic crust that are engulfed in a sea of Ediacaran granites and related dikes and volcanic rocks.
4. In the NE Desert, remnants of Cryogenian and Tonian crust are engulfed in a sea of Ediacaran granites and related dikes and volcanic rocks.
5. Cryogenian and Late Tonian sequences are spectacularly exposed in the Central ED. Relationships between infracrustal gneisses and mesozonal granitic rocks structurally overlain by Late Tonian–Cryogenian ophiolites and distinctive sediments especially banded iron formation and Atud diamictite are locally preserved where they are not disrupted by Ediacaran shear zones of the Najd system, cut by abundant Ediacaran granites, or buried beneath Ediacaran terrestrial sediments of the Hammamat Group. Widespread carbonatization and gold mineralization also characterize the CED.
6. Infrastructure gneisses and intrusives in CED and SED are mistakenly thought to be pre-Neoproterozoic "fundamental basement" but these are clearly represent juvenile middle crust that formed in Neoproterozoic time, as shown by radiometric and isotopic investigations.
7. Basement exposed in the SED covers a much larger area and is much less studied than the basement exposures of Sinai, the NED or the CED. SED basement shares many petrologic characteristics like that of the CED including abundance of ophiolites and gneisses. Limited geochronologic data suggests that it is generally slightly older than the CED; the SED is less affected by Najd shearing than is the CED. Much more work is needed to better understand SED crustal evolution, especially zircon geochronology and related studies. The SED represents one frontier of Egyptian basement geology.
8. The only well-preserved suture in Egypt is the E-W trending Allaqi-Heiani-Gerf-Onib ophiolite belt. ~730 Ma ophiolites were emplaced during terrane collision ~700 Ma.
9. A glimpse of older basement is provided by scattered outcrops along the E-W trending Nubian Swell, just N of the Sudan border. The boundary between juvenile crust of the Arabian-Nubian Shield in the east and the Saharan Metacraton in the west is marked by a broad zone of Neoproterozoic granites and gneisses with isotopic compositions indicating reworking of older crust. West of this transition zone are extensive outcrops of Archean and Paleoproterozoic rocks in the far SW of the Western Desert.
10. We need to find ways to obtain and study samples of Precambrian basement buried beneath Phanerozoic sediments west of the Eastern Desert and north of the Nubian Swell. Future efforts to understand this crust will require co-operation between industrial and academic geophysicists and geologists. Geophysical studies will be very useful for understanding the large scale crustal structure of this region. Exploration of this "last frontier" is likely to reveal some surprising results.

Acknowledgements Thanks to Ghaleb Jarrar (U. Jordan) for help understanding the basement of SW Jordan, to Dov Avigad (Hebrew U.) for help understanding the basement of southernmost Israel, Hassan Helmy (El Minia U.) for help understanding SE Desert mafic-ultramafic intrusions. We appreciate critical comments and suggestions of two anonymous referees. This is UTD Geosciences contribution # 1339.

References

Abdeen MM, Greiling RO (2005) A quantitative structural study of late Pan-African compressional deformation in the central eastern desert (Egypt) during Gondwana assembly. Gondwana Res 8:457–471

Abdel Halim AH, Helmy HM, Abd El-Rahman YM, Shibata T (2016) Petrology of the motaghairat mafic-ultramafic complex, Eastern Desert, Egypt: a high-Mg post-collisional extension-related layered intrusion. J Asian Earth Sci 116:164–180

Abdel-Karim A-AM, Ahmed Z (2010) Possible origin of the ophiolites of Eastern Desert, Egypt, from geochemical perspectives. Arab J Sci Eng 35:115–143

Abdel-Karim AAM, Ali S, Helmy HA, El-Shafei SA (2016) A fore-arc setting of the Gerf ophiolite, Eastern Desert, Egypt: evidence from mineral chemistry and geochemistry of ultramafites. Lithos 263:52–65

Abdelsalam MG, Abdeen MM, Dowaidar HM, Stern RJ, Abdelghaffar AA (2003) Structural evolution of the Neoproterozoic Western Allaqi–Heiani suture, southeastern Egypt. Precambr Res 124:87–104

Abdelsalam MG, Liégeois JP, Stern RJ (2002) The Saharan Metacraton. J Afr Earth Sci 34:119–136

Abdel-Rahman AFM, Doig R (1987) The Rb-Sr geochronological evolution of the Ras Gharib segment of the Northern Nubian Shield. J Geol Soc Lond 144:577–586

Abd El-Rahman Y, Polat A, Dilek Y, Fryer BJ, El-Sharkawy M, Sakran S (2009a) Geochemistry and tectonic evolution of the Neoproterozoic incipient arc–forearc crust in the Fawakhir area, Central Eastern Desert of Egypt. Precambr Res 175:116–134

Abd El-Rahman Y, Polat A, Dilek Y, Fryer BJ, El-Sharkawy M, Sakran S (2009b) Geochemistry and tectonic evolution of the Neoproterozoic Wadi Ghadir ophiolite, Eastern Desert, Egypt. Lithos 113:158–178

Abd El-Rahman Y, Seifert T, Gutzmer J, Said A, Hofmann M, Gärtner A, Linnemann U (2017) The south Um Mongol Cu-Mo-Au prospect in the Eastern Desert of Egypt: from a mid-Cryogenian continental arc to Ediacaran post-collisional appinite-high Ba-Sr monzogranite. Ore Geol Rev 80:250–266

Abd El-Rahman Y, Surour AA, El-Manawi AHW, El-Dougdoug A-MA, Omar S (2015) Regional setting and characteristics of the Neoproterozoic Wadi Hamama Zn-Cu-Ag-Au prospect: evidence for an intra-oceanic island arc-hosted volcanogenic hydrothermal system. Int J Earth Sci 104:625–644

Abu-Alam TS, Stüwe K (2009) Exhumation during oblique transpression: the Feiran-Solaf region. Egypt J Metamorph Geol 27:439–459

Abu El-Enen MM, Whitehouse MJ (2013) The Feiran-Solaf metamorphic complex, Sinai, Egypt: geochronological and geochemical constraints on its evolution. Precambr Res 239:106–125

Abu El-Enen M, Will TM, Okrusch M (2004) P–T evolution of the Pan-African Taba metamorphic belt, Sinai, Egypt: constraints from metapelitic mineral assemblages. J Afr Earth Sci 38:59–78

Agrinier P, Mével C, Bosch D, Javoy M (1993) Metasomatic hydrous fluids in amphibole peridotites. Earth Planet Sci Lett 120:187–205

Ali KA, Azer MK, Gahlan HA, Wilde SA, Samuel MD, Stern RJ (2010a) Age constraints on the formation and emplacement of Neoproterozoic ophiolites along the Allaqi–Heiani Suture, South Eastern Desert of Egypt. Gondwana Res 18:583–595

Ali KA, Stern RJ, Manton WI, Kimura J-I, Khamis HA (2009) Geochemistry, Nd isotopes, and U-Pb SHRIMP zircon dating of Neoproterozoic volcanic rocks from the Central Eastern Desert of Egypt: new insights into the ~750 Ma crust-forming event. Precambr Res 171:1–22

Ali KA, Stern RJ, Manton WI, Johnson PR, Mukherjee SK (2010b) Neoproterozoic diamictite in the Eastern Desert of Egypt and Northern Saudi Arabia: evidence of ~750 Ma glaciation in the Arabian-Nubian Shield. Int J Earth Sci 90:705–726

Ali KA, Kröner A, Hegner E, Wong J, Li S-Q, Gahlan HA, El Ela FF (2015) U-Pb zircon geochronology and Hf–Nd isotopic systematics of Wadi Beitan granitoid gneisses, South Eastern Desert, Egypt. Gondwana Res 27:811–824

Ali KA, Zoheir BA, Stern RJ, Andresen A, Whitehouse MJ, Bishara WW (2016) Lu-Hf and O isotopic compositions on single zircons from the North Eastern Desert of Egypt, Arabian-Nubian Shield: implications for crustal evolution. Gondwana Res 32:181–192

Ali-Bik MW, Sadek MF, Ghabrial DS (2014) Late Neoproterozoic metamorphic assemblages along the Pan-African Hamisana Shear Zone, southeastern Egypt: metamorphism, geochemistry and petrogenesis. J Afr Earth Sci 99:24–38

Ali-Bik MW, Abd El Rahim SH, Abdel Wahab W, Abayazeed SD, Hassan SM (2017) Geochemical constraints on the oldest arc rocks of the Arabian-Nubian Shield: the late Mesoproterozoic to Late Neoproterozoic (?) Sa'al volcano-sedimentary complex, Sinai, Egypt. Lithos 284–285:310–326

Andresen A, El-Enen MM, Stern RJ, Wilde SA, Ali KA (2014) The Wadi Zaghra metasediments of Sinai, Egypt: new constraints on the late Cryogenian–Ediacaran evolution of the northernmost Arabian-Nubian Shield. Int Geol Rev 56:1020–1038

Andresen A, Abu El-Rus MA, Myhre PI, Boghdady GY, Corfu F (2009) U-Pb TIMS age constraints on the evolution of the Neoproterozoic Meatiq Gneiss Dome, Eastern Desert of Egypt. Int J Earth Sci 98:481–497

Augland LE, Andresen A, Boghdady GY (2012) U-Pb ID-TIMS dating of igneous and metaigneous rocks from the El-Sibai area: time constraints on the tectonic evolution of the Central Eastern Desert, Egypt. Int J Earth Sci 101:25–37

Avigad D, Gvirtzman Z (2009) Late Neoproterozoic rise and fall of the northern Arabian-Nubian Shield: the role of lithospheric mantle delamination and subsequent thermal subsidence. Tectonophysics 477:217–228

Avigad D, Weissbrod T, Gerdes A, Zlatkin O, Ireland TR, Morag N (2015) The detrital zircon U-Pb-Hf fingerprint of the northern Arabian-Nubian Shield as reflected by a Late Ediacaran arkosic wedge (Zenifim Formation; subsurface Israel). Precambr Res 266:1–11

Azer MK, Gahlan HA, Asimow PD, Al-Kahtany K (2017) The Late Neoproterozoic Dahanib Mafic-ultramafic intrusion, south-eastern desert, Egypt: is it an Alaskan-type or layered intrusion? Am J Sci 317:91–940

Azer M, Obeid MA, Ren M (2014) Geochemistry and petrogenesis of late Ediacaran (605–580 Ma) post-collisional alkaline rocks from the Katherina ring complex, south Sinai, Egypt. J Asian Earth Sci 93:229–252

Azer MK, Samuel MD, Ali KA, Gahlan HA, Stern RJ, Ren M, Moussa HE (2013) Neoproterozoic ophiolitic peridotites along the Allaqi–Heiani suture, South Eastern Desert, Egypt. Mineral Petrol 107:829–848

Azer MK, Stern RJ (2007) Neoproterozoic (835–720 Ma) serpentinites in the Eastern Desert, Egypt: fragments of forearc mantle. J Geol 115:457–472

Azer MK, Stern RJ, Kimura JI (2010) Origin of a Late Neoproterozoic (605 ± 13 Ma) intrusive carbonate–albitite complex in southern Sinai, Egypt. Int J Earth Sci 99:245–267

Bea F, Abu-Anbar M, Montero P, Peres P, Talavera C (2009) The ~844 Ma Moneiga quartz-diorites of the Sinai, Egypt: evidence for

Andean-type arc or rift-related magmatism in the Arabian-Nubian Shield? Precambr Res 175:161–168
Bea F, Montero P, Abu Anbar M, Molina JF, Scarrow JH (2011a) The Bir Safsaf Precambrian inlier of South West Egypt revisited. A model for ~1.5 Ga T_{DM} late Pan-African granite generation by crustal reworking. Lithos 125:897–914
Bea F, Montero P, Abu Anbar M, Talavera C (2011b) SHRIMP dating and Nd isotope geology of the Archean terranes of the Uweinat-Kamil inlier, Egypt–Sudan–Libya. Precambr Res 189:328–346
Be'eri-Shlevin Y, Katzir Y, Valley JW (2009a) Crustal evolution and recycling in a juvenile continent: oxygen isotope ratio of zircon in the northern Arabian-Nubian Shield. Lithos 107:169–184
Be'eri-Shlevin Y, Katzir Y, Whitehouse M (2009b) Post-collisional tectonomagmatic evolution in the northern Arabian-Nubian Shield (ANS): time constraints from ion-probe U-Pb dating of zircon. J Geol Soc Lond 166:71–85
Be'eri-Shlevin Y, Eyal M, Eyal Y, Whitehouse MJ, Litvinovsky B (2012) The Sa'al volcano-sedimentary complex (Sinai, Egypt): a latest Mesoproterozoic volcanic arc in the northern Arabian Nubian Shield. Geology 40:403–406
Bennett GD, Mosely P (1987) Tiered tectonics and evolution, Eastern Desert and Sinai, Egypt. In: Matheis G, Schandelmeier H (eds) Current research in African Earth sciences. Balkema, Rotterdam, The Netherlands, pp 79–82
Bernau R, Darbyshire DPF, Franz G, Harms U, Huth A, Mansour N, Pasteels P, Schandelmeier H (1987) Petrology, geochemistry, and structural development of the Bir Safsaf-Aswan uplift, Southern Egypt. J Afr Earth Sci 6:79–90
Boskabadi A, Pitcairn IK, Broman C, Boyce A, Teagle DAH, Cooper MJ, Azer MK, Mohamed FH, Stern RJ (2016) Carbonate alteration of ophiolitic rocks in the Arabian Nubian Shield of Egypt: sources and compositions of the carbonating fluid and implications for the formation of Au deposits. Int Geol Rev 59:391–419
Boudier F, Nicolas A, Kienast JR, Mevel C (1988) The gneiss of Zabargad island: deep crust of rift. Tectonophysics 150:209–227
Breitkreuz C, Eliwa H, Khalaf I, El Gameel K, Bühler B, Sergeev S, Larionov A (2010) Neoproterozoic SHRIMP U-Pb zircon ages of silica-rich Dokhan Volcanics in the northeastern Desert, Egypt. Precambr Res 182:163–174
Brueckner HK, Elhaddad MA, Hamelin B, Hemmings S, Kröner A, Reisberg L, Seyler M (1995) A Pan African origin and uplift for the gneisses and peridotites of Zabargad Island, Red Sea: a Nd, Sr, Pb, and Os isotope study. J Geophys Res Solid Earth 100:22283–22297
Bühler B, Breitkreuz C, Pfänder JA, Hofmann M, Becker S, Linnemann U, Eliwa HA (2014) New insights into the accretion of the Arabian-Nubian Shield: depositional setting, composition and geochronology of a mid-Cryogenian arc succession (North Eastern Desert, Egypt). Precambr Res 243:149–167
de Wall H, Greiling RO, Sadek MF (2001) Post-collisional shortening in the late Pan-African Hamisana high strain zone, SE Egypt: field and magnetic fabric evidences. Precambr Res 107:179–194
Dixon TH (1981a) Gebel Dahanib, Egypt: a late Precambrian layered sill of komatiitic composition. Contrib Miner Petrol 76:42–53
Dixon TH (1981b) Age and chemical characteristics of some pre-Pan-African rocks in the Egyptian Shield. Precambr Res 14:119–133
El Bahariya GA (2018) Classification of the Neoproterozoic ophiolites of the Central Eastern Desert, Egypt based on field geological characteristics and mode of occurrence. Arab J Geosci 11:313. https://doi.org/10.1007/s12517-018-3677-1
El-Nisr SA (1997) Late Precambrian volcanism at Wadi Allaqi, south Eastern Desert, Egypt: evidence for transitional continental arc/margin environment. J Afr Earth Sci 24:301–312
El-Shazly AK, Khalil KI (2014) Banded iron formations of Um Nar, Eastern Desert of Egypt: P-T-X conditions of metamorphism and tectonic implications. Lithos 196–197:356–375
Eliwa HA, Breitkreuz C, Murata M, Khalaf IM, Bühler B, Itaya T, Takahashi T, Hirahara Y, Miyazaki T, Kimura J-I, Shibata T, Koshi Y, Kato Y, Ozawa H, Daas MA, El Gameel KH (2014) SIMS zircon U-Pb and mica K–Ar geochronology, and Sr–Nd isotope geochemistry of the north Eastern Desert, Egypt. Gondwana Res 25:1570–1598
Eliwa H, Kimura J-I, Itaya T (2006) Late Neoproterozoic Dokhan Volcanics, North Eastern Desert, Egypt: geochemistry and petrogenesis. Precambr Res 151:31–52
Eyal M, Bartov Y, Shimron AE, Bentor YK (1980) Sinai geological map, aeromagnetic map. Survey of Israel, Scale: 1:500 000, 1 sheet
Eyal M, Be'eri-Shlevin Y, Eyal Y, Whitehouse MJ, Litvinovsky B (2014) Three successive Proterozoic island arcs in the Northern Arabian-Nubian Shield: evidence from SIMS U-Pb dating of zircon. Gondwana Res 25:338–357
Eyal M, Livinovsky B, Jahn BM, Zanvillevich A, Katzir Y (2010) Origin and evolution of post-collisional magmatism: coeval calc-alkaline and alkaline suites of the sinai Peninsula. Chem Geo 269:153–179
Farahat ES (2010) Neoproterozoic arc–back-arc system in the Central Eastern Desert of Egypt: evidence from supra-subduction zone ophiolites. Lithos 120:293–308
Finger F, Dörr W, Gerdes A, Gharib M, Dawoud M (2008) U-Pb zircon ages and geochemical data for the Monumental Granite and other granitoid rocks from Aswan, Egypt: implications for the geological evolution of the western margin of the Arabian-Nubian Shield. Miner Petrol 93:153–183
Fowler A, Hassan IS, Hassan M (2018) The Feiran-Solaf metamorphic complex, Sinai, Egypt: evidence for orthogonal or oblique tectonic convergence? J Afr Earth Sci 46:48–65
Fowler A-R, El Kalioubi B (2002) The Migif-Hafafit gneissic complex of the Egyptian Eastern Desert: fold interference patterns involving multiply deformed sheath folds. Tectonophysics 346:247–275
Fowler A, Osman AF (2013) Sedimentation and inversion history of three molasse basins of the western Central Eastern Desert of Egypt: implications for the tectonic significance of Hammamat basins. Gondwana Res 23:1511–1534
Gahlan HA, Azer MK, Khalil AES (2015) The Neoproterozoic Abu Dahr ophiolite, South Eastern Desert, Egypt: petrological characteristics and tectonomagmatic evolution. Mineral Petrol 109:611–630
Gindy AR, Tamish MM (1998) Petrogenetic revision of the basement rocks in the environs of Aswan, southern Egypt. Egypt J Geol 42:1–14
Hamimi Z, Abd El-Wahed MA, Gahlan HA, Kamh SZ (2019) Tectonics of the Eastern Desert of Egypt: key to understanding the Neoproterozoic evolution of the Arabian-Nubian Shield. In: Bendaoud A et al (eds) The geology of the Arab world—an overview. Springer Geology. https://doi.org/10.1007/978-3-319-96794-3_1
Harris NBW, Hawkesworth CJ, Ries AC (1984) Crustal evolution in north-east and east Africa from model Nd ages. Nature 309:773–776
Helmy HM (1999) The Um Samiuki volcanogenic Zn-Cu-Pb-Ag deposit, Eastern Desert: a possible new occurrence of Cervelleite. Can Mineral 37:143–158
Helmy HM (2004) Cu-Ni-PGE mineralization in the Genina Gharbia mafic-ultramafic intrusion, Eastern Desert, Egypt. Can Mineral 42:351–370
Helmy HM, Abd El-Rahman YM, Yoshikawa M, Shibata T, Arai S, Tamura A, Kagami H (2014) Petrology and Sm-Nd dating of the Genina Gharbia Alaskan-type complex (Egypt): insights into deep levels of Neoproterozoic island arcs. Lithos 198–199:263–280

Helmy HM, El Mahallawi MM (2003) Gabbro Akarem mafic-ultramafic complex, Eastern Desert, Egypt: a Late Precambrian analogues of Alaskan-type complexes. Miner Petrol 77:85–108

Hosny A, Nyblade A (2016) Crustal structure of Egypt from Egyptian National Seismic Network data. Tectonophysics 687:257–267

Helmy HM, Yoshikawa M, Shibata T, Arai S, Kagami H (2015) Sm-Nd and Rb-Sr isotope geochemistry and petrology of Abu Hamamid intrusion, Eastern Desert of Egypt: an Alaskan-type complex in a backarc setting. Precambr Res 258:234–246

Helmy H, Zoheir B (2015) Metal and fluid sources in a potential world-class gold deposit: El-Sid mine, Egypt. Int J Earth Sci 104:645–661

Jarrar GH, Theye T, Yaseen N, Whitehouse M, Pease V, Passchier C (2013) Geochemistry and P-T-t evolution of the Abu-Barqa Metamorphic Suite, SW Jordan, and implications for the tectonics of the northern Arabian-Nubian Shield. Precambr Res 239:56–78

Johnson PR, Woldhaimanot B (2003) Development of the Arabian-Nubian Shield: perspectives on accretion and deformation in the northern East African Orogen and the assembly of Gondwana. In: Yoshida M, Dasgupta S, Windley B (eds) Proterozoic East Gondwana: supercontinent assembly and breakup. Special Pub. 206. Geological Society of London, pp 289–325

Karmakar S, Schenk V (2015) Neoarchean UHT metamorphism and Paleoproterozoic UHT Reworking at Uweinat in the East Sahara Ghost Craton, SW Egypt: evidence from petrology and texturally controlled in situ Monazite dating. J Petrol 56:1703–1742

Katzir Y, Litvinovsky BA, Jahn BM, Eyal M, Zanvilevich AN, Valley JW, Vapnik Y, Beeri Y, Spicuzza MJ (2007) Interrelationships between coeval mafic and A-type silicic magmas from composite dykes in a bimodal suite of southern Israel, northernmost Arabian-Nubian Shield: geochemical and isotope constraints. Lithos 97:335–364

Khalil AES, Azer MK (2007) Supra-subduction affinity in the Neoproterozoic serpentinites in the Eastern Desert, Egypt: evidence from mineral composition. J. Afr Earth Sci 49:136–152

Kröner A, Eyal M, Eyal Y (1990) Early Pan-African evolution of the basement around Elat, Israel, and the Sinai Peninsula revealed by single-zircon evaporation dating, and implications for crustal accretion rates. Geology 18:545–548

Kröner A, Krüger J, Rashwan AAA (1994) Age and tectonic setting of granitoid gneisses in the Eastern Desert of Egypt and south-west Sinai. Geol Rundsch 83:502–513

Kröner A, Todt W, Hussein IM, Mansour IM, Mansour M, Rashwan AA (1992) Dating of late Proterozoic ophiolites in Egypt and the Sudan using the single grain zircon evaporation technique. Precambr Res 59:15–32

Lancelot JR, Bosch D (1991) A Pan African age for the HP-HT granulite gneisses of Zabargad island: implications for the early stages of the Red Sea rifting. Earth Planet Sci Lett 107:539–549

Liégeois J-P, Stern RJ (2010) Sr-Nd isotopes and geochemistry of granite-gneiss complexes from the Meatiq and Hafafit domes, Eastern Desert, Egypt: no evidence for pre-Neoproterozoic crust. J Afr Earth Sci 57:31–40

Morag N, Avigad D, Gerdes A, Belousova E, Harlavan Y (2011) Crustal evolution and recycling in the northern Arabian-Nubian Shield: new perspectives from Late Neoproterozoic sediments (Elat area, Israel). Precambr Res 186:101–116

Morag N, Avigad D, Gerdes A, Harlavan Y (2012) 1000–580 Ma crustal evolution in the northern Arabian-Nubian Shield revealed by U-Pb-Hf of detrital zircons from Late Neoproterozoic sediments (Elat area, Israel). Precambr Res 208–211:197–212

Moghazi A-KM, Ali KA, Wilde SA, Zhou Q, Andersen T, Andresen A, Abu El-Enen MM, Stern RJ (2012) Geochemistry, geochronology, and Sr-Nd isotopes of the Late Neoproterozoic Wadi Kid volcano-sedimentary rocks, southern Sinai, Egypt: implications for tectonic setting and crustal evolution. Lithos 154:147–165

Moussa EMM, Stern RJ, Manton WI, Ali KA (2008) SHRIMP zircon dating and Sm/Nd isotopic investigations of Neoproterozoic granitoids, Eastern Desert, Egypt. Precambr Res 160: 341–356

Powell JH, Abed AA, Le Nidre Y-M (2014) Cambrian stratigraphy of Jordan. GeoArabia 19:81–134

Ries AC, Shackleton RM, Graham RH, Fitches WR (1983) Pan-African structures, opiolites and mélange in the Eastern Desert of Egypt: a traverse at 26°N. J Geol Soc London 140:75–95

Samuel MD, Be'eri-Shlevin Y, Azer MK, Whitehouse MJ, Moussa HE (2011) Provenance of conglomerate clasts from the volcani-sedimentary sequence at Wadi Rutig in southern Sinai, Egypt as revealed by SIMS U-Pb dating of zircon. Gondwana Res 20:450–464

Shalaby A (2010) The northern dome of Wadi Hafafit culmination, Eastern Desert, Egypt: structural setting in tectonic framework of a scissor-like wrench corridor. J Afr Earth Sci 57:227–241

Sims PK, James HL (1984) Banded iron-formation of Late Proterozoic age in the Central Eastern Desert, Egypt: geology and tectonic setting. Econ Geol 79:1777–1784

Stern RJ (1981) Petrogenesis and tectonic setting of late Precambrian ensimatic volcanic rocks, Central Eastern Desert of Egypt. Precambr Res 16:195–230

Stern RJ (1985) The Najd fault system, Saudi Arabia and Egypt: a Late Precambrian rift–related transform system. Tectonics 4:497–511

Stern RJ (2018) Neoproterozoic formation and evolution of Eastern Desert Continental Crust—the importance of the infrastructure-superstructure transition. J Afr Earth Sci 18:15–27

Stern RJ, Ali KA, Liégeois J-P, Johnson P, Wiescek F, Kattan F (2010a) Distribution and significance of pre-Neoproterozoic Zircons in Juvenile Neoproterozoic igneous rocks of the Arabian-Nubian Shield. Am J Sci 310:791–811

Stern RJ, Ali K, Ren M, Jarrar GH, Romer RL, Leybourne M, Whitehouse MJ (2016a) Cadomian (~560 Ma) crust buried beneath the Northern Arabian Peninsula: mineral, chemical, geochronological, and isotopic constraints from NE Jordan xenoliths. Earth Planet Sci 436:31–42

Stern RJ, Ali K, Ren M, Jarrar GH, Romer RL, Leybourne M, Whitehouse MJ (2016b) Cadomian (~560 Ma) crust buried beneath the Northern Arabian Peninsula: mineral, chemical, geochronological, and isotopic constraints from NE Jordan xenoliths. Earth Planet Sci 436:31–42

Stern RJ, Gottfried D, Hedge CE (1984) Late Precambrian rifting and crustal evolution in the Northeastern Desert of Egypt. Geology 12:168–171

Stern RJ, Hedge CE (1985) Geochronologic constraints on late Precambrian crustal evolution in the Eastern Desert of Egypt. Am J Sci 285:97–127

Stern RJ, Ali KA, Liégeois J-P, Johnson P, Wiescek F, Kattan F (2010b) Distribution and Significance of pre-Neoproterozoic Zircons in Juvenile Neoproterozoic Igneous Rocks of the Arabian-Nubian Shield. Am J Sci 310:791–811

Stern RJ, Johnson P (2010) Continental lithosphere of the Arabian plate: a geologic, petrologic, and geophysical synthesis. Earth Sci Rev 101:29–67

Stern RJ, Kröner A, Manton WI, Reischmann T, Mansour M, Hussein IM (1989) Geochronology of the late Precambrian Hamisana shear zone, Red Sea Hills, Sudan and Egypt. J Geol Soc 146:1017–1029

Stern RJ, Kröner A, Rashwan AA (1991) A Late Precambrian (~710 Ma) high volcanicity rift in the souther Eastern Desert of Egypt. Geol Rundsch 80(1):155–170

Stern RJ, Manton WI (1987) Age of Feiran basement rocks, Sinai: implications for late Precambrian evolution in the northern Arabian-Nubian Shield. J Geol Soc Lond 144:569–575

Stern RJ, Mukherjee SK, Miller NR, Ali K, Johnson PR (2013) banded iron formation from the Arabian-Nubian Shield—implications for understanding Neoproterozoic climate change. Precambr Res 239:79–94

Stern RJ, Nielsen KC, Best E, Sultan M, Arvidson RE, Kröner A (1990) Orientation of late Precambrian sutures in the Arabian-Nubian Shield. Geology 18:1103–1106

Stern RJ, Ren M, Ali K, Förster H-J, Al Safarjalani A, Nasir S, Whitehouse MJ, Leybourne MI (2014) Early Carboniferous (~357 Ma) crust beneath northern Arabia: tales from Tell Thannoun (southern Syria). Earth Planet Sci Lett 393:83–93

Stern RJ, Sellers G, Gottfried D (1988) Bimodal dike swarms in the Northeastern Desert of Egypt: significance for the origin of late Precambrian 'A-Type' granites in northern Afro–Arabia. In: Greiling R, El Gaby S (eds) The Pan-African belt of NE Africa and Adjacent Areas: tectonic evolution and economic aspects, pp 147–179

Stern RJ, Voegeli DA (1987) Geochemistry, geochronology, and petrogenesis of a late Precambrian (~590 Ma) composite dike from the North Eastern Desert of Egypt. Geol Rundsch 76:325–341

Sultan M, Arvidson RE, Sturchio NC (1986) Mapping of serpentinites in the Eastern Desert of Egypt by using Landsat thematic mapper data. Geology 14:995–999

Sultan M, Chamberlain KC, Bowring SA, Arvidson RE, Abuzeid H, El Kaliouby B (1990) Geochronologic and isotopic evidence for involvement of pre-Pan-African crust in the Nubian shield, Egypt. Geology 18:761–764

Sultan M, Tucker RD, El Alfy Z, Attia R (1994) U-Pb (zircon) ages for the gneissic terrane west of the Nile, southern Egypt. Geol Rundsch 83:514–522

Thurmond AK, Stern RJ, Abdelsalam MG, Nielsen KC, Abdeen MM, Hinz E (2004) The Nubian Swell. J Afr Earth Sci 39:401–407

Walker JD, Geissman JW, Bowring SA, Babcock LE (2012) Geologic Time Scale v. 4.0, Geological Society of America

Wilde, SA, Youssef, K (2000) Significance of SHRIMP U–Pb dating of the Imperial Porphyry and associated Dokhan Volcanics, Gabal Dokhan, North Eastern Desert, Egypt. J Afr Earth Sci 31:403–413

Zimmer M, Kröner A, Jochum KP, Reischmann T, Todt W (1995) The Gabal Gerf: a precambrian N-MORB ophiolite in the Nubian Shield, NE Africa. Chem Geol 123:29–51